PHYSICAL REVIEW B VOLUME 42, NUMBER 16 1 DECEMBER 1990

# Exact theories of $m$-component quadrupolar systems showing a first-order phase transition

Kaoru Ohno[*]
*Department of Physics, College of General Education, Tohoku University, Kawauchi, Sendai, Miyagi 980, Japan*

Hans-Otto Carmesin[†]
*Courant Institute of Mathematical Sciences, New York University, New York, New York 10012*
*and Department of Chemistry, State University of New York, Albany, New York 12222*

Hikaru Kawamura
*Department of Physics, College of General Education, Osaka University, Toyonaka, Osaka 560, Japan*

Yutaka Okabe
*Department of Physics, Faculty of Science, Tohoku University, Aoba, Sendai, Miyagi 980, Japan*

(Received 1 May 1990; revised manuscript received 27 August 1990)

Several statistical-thermodynamic theories involving an exact solution in one dimension ($d=1$), high- and low-temperature series expansions, and an exact solution of an infinite-range system (mean-field theory) are presented for a quadrupolar spin model whose Hamiltonian is described with $m$-component classical spins $\mathbf{S}_i$ as $\mathcal{H}=-\frac{1}{2}\sum_{i,j=1}^{N}J_{ij}(\mathbf{S}_i\cdot\mathbf{S}_j)^2$ on a $d$-dimensional lattice. An orientational phase transition is analyzed systematically as a function of $m$. The transition is first order generally for $2<m\leq\infty$ and $d>2$. We evaluate the transition point and the discontinuity in energy as a function of $m$. We also present exact solutions in the $m\to\infty$ limit for arbitrary spatial dimensions.

## I. INTRODUCTION

In molecular crystals and liquid crystals, interactions between nonspherical molecules are generally complicated and depend on mutual angles and distances of the molecules. If the molecules have no dipole component, i.e., no polarity, and have an oval shape (Fig. 1), it is understood that the interactions can be expanded in Legendre series with even orders. When the lowest term proportional to $P_2(\cos\theta_{ij})$ dominates the other terms in the expansion, i.e., when the molecules are well approximated as uniaxial quadruples, the system of this molecular crystal is described by a Hamiltonian:

$$\mathcal{H}=\mathcal{H}_0-\tfrac{1}{2}\sum_{i,j=1}^{N}J(r_{ij})\cos^2\theta_{ij}\ , \tag{1.1}$$

where $\mathcal{H}_0$ is a constant, $r_{ij}$ and $\theta_{ij}$ are distance and angle between two molecules $i$ and $j$. This model was first discussed by Maier and Saupe[1] for the isotropic-nematic phase transition of liquid crystals. Let us introduce classical $m$-component spin variables

$$\mathbf{S}_i=(S_i^1,S_i^2,\ldots,S_i^m),\quad |\mathbf{S}_i|=S_0 \tag{1.2}$$

with $i=1,2,\ldots,N$ ($N$ is the total number of sites). For simplicity we introduce a $d$-dimensional lattice, fixing each spin on each lattice site and ignoring any spatial displacement. This simplification would be valid in discussing the property of the orientational phase transition, if no spatial order switches on simultaneously at the transition point. Then one may rewrite the above Hamiltonian in a form

$$\mathcal{H}=-\tfrac{1}{2}\sum_{i,j=1}^{N}J_{ij}(\mathbf{S}_i\cdot\mathbf{S}_j)^2 \tag{1.3}$$

apart from constant $\mathcal{H}_0$. We call this Hamiltonian system an $m$-component quadrupolar system. If the interactions act between only nearest-neighbor spins with an equal strength $J_{ij}=J$, the Hamiltonian (1.3) reduces to

$$\mathcal{H}_{\text{quadrupole}}=-J\sum_{\substack{\langle ij\rangle\\(1\leq i,j\leq N)}}(\mathbf{S}_i\cdot\mathbf{S}_j)^2\ . \tag{1.4}$$

This model should be compared with the standard $m$-vector model whose Hamiltonian is given by

$$\mathcal{H}_{\text{vector}}=-G\sum_{\substack{\langle ij\rangle\\(1\leq i,j\leq N)}}\mathbf{S}_i\cdot\mathbf{S}_j\ . \tag{1.5}$$

The quadrupolar model described by (1.4) is equivalent to the $\mathrm{RP}^{m-1}$ model in field theory.[2] It is possible, in prin-

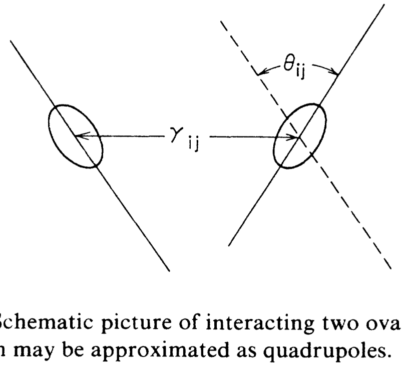

FIG. 1. Schematic picture of interacting two oval-shape molecules which may be approximated as quadrupoles.

ciple, to consider a mixed Hamiltonian which has both the quadrupolar part (1.4) and the vector part (1.5). In this case, the vector part plays a role of a symmetry breaking field along the director axis. Such a mixed Hamiltonian may describe annealed magnets or some kind of liquid or molecular crystals.[3] On the other hand, usual orientational orderings associated with the rotational symmetry breaking are characterized by a quadrupolar order parameter

$$\Delta^{\mu\nu}=\left\langle \left[ S_i^{\mu} S_i^{\nu} - S_0^2 \frac{\delta_{\mu\nu}}{m} \right] \right\rangle , \tag{1.6}$$

which is traceless, i.e., $\sum_{\mu} \Delta^{\mu\mu}=0$. The field associated with this order parameter is not (1.5) but

$$\mathcal{H}_{\text{field}} = - \sum_{i=1}^{N} \sum_{\mu,\nu=1}^{m} H^{\mu\nu} S_i^{\mu} S_i^{\nu} . \tag{1.7}$$

(Inclusion of such a term will be treated later in an exact manner both for general $m$ in an infinite-range system and for the $m \rightarrow \infty$ limit in a short-range system.) Although it is possible to further generalize the Hamiltonian by considering quadrupolar glasses,[4,5] where $J_{ij}$ is spatially random in (1.3), or chiral transitions,[6] we restrict ourselves basically to the simplest case of the homogeneous quadrupolar models in the following.

The $m=1$ quadrupolar model is trivial at a first glance, because the Hamiltonian becomes always constant in this case, although the limit $m \rightarrow 1$ might have some meaning. The $m=2$ model is equivalent to the classical $X$-$Y$ model (planar model) which undergoes a second-order phase transition,[7] because of an identity $\cos^2\theta_{ij}=(1+\cos 2\theta_{ij})/2$. How about the case of larger values of $m$? One may find just from symmetry considerations that possible phase transition is first order for general numbers of spin components.[8,9] A Monte Carlo study[10] has been carried out for $m=3$ in three dimensions and exhibited indeed a first-order phase transition at finite temperature $T_c$. There are also several important works in two dimensions.[11-13] In two dimensions, much interest has been aroused in vortex condensations and topological orderings.[11]

As far as we know, however, there was so far no report studying systematic $m$-dependences of general $m$-component quadrupolar systems. The main purpose of this paper is to discuss the order of phase transitions and give reliable estimates for the transition point as a function of $m$ (and also for the discontinuity at that point if the transition is first order). In this paper we present several exact or rigorous theories of $m$-component quadrupolar models. Especially, we give a complete analysis including an exact solution in $d=1$ of a short-range system and an exact solution in arbitrary dimensions of an infinite-range system which corresponds to mean-field theory. We find that the short-range system at $d=1$ shows a second-order phase transition in the $m \rightarrow \infty$ limit and no phase transition for any finite values of $m$. While, in the analysis of the infinite-range system, we find that the transition is first order for all $m < 2 \leq \infty$.

The knowledge of these exact solutions helps us to develop high- and low-temperature series expansions of the present model with a short-ranged interaction. The high-temperature expansion is essentially a (graphical) linked cluster expansion. We notice that there are two theorems with which weight functions associated with spin traces for higher order graphs can easily be calculated from lower order graphs. In fact we need to evaluate only nine independent spin integrals in order to obtain a result up to the seventh order in a simple cubic lattice. On the other hand, the low-temperature series expansion is possible at arbitrary spatial dimension $d$ although a restriction, $d>2$, should be imposed for the existence of an orientationally ordered phase. For the nearest-neighbor model (1.4) we will present explicitly the high-temperature series up to the seventh order and the low-temperature series up to the second order for general values of $m$. Then, from these series data, we conclude that a first-order transition generally takes place for $m>2$ in three spatial dimensions. It is also possible to estimate the transition temperature $T_c$ and the discontinuity of the internal energy $\Delta E_c$.

We pay further attention to exact solutions in the large-$m$ limit not only for completeness to all $m$ but also for simplicity of these solutions which are described just by elementary functions. For an infinite-range case we find, in this limit, a single first-order phase transition associated with the orientational ordering. On the other hand, in a short-range case, Kunz and Zumbach[14] obtained quite recently an exact solution of the $\mathrm{RP}^{m-1}$ model in the $m \rightarrow \infty$ limit which shows a first-order phase transition for $d \geq 2$. We reanalyzed this limit in terms of the quadrupolar model by explicitly taking account of an effect of symmetry breaking fields (1.5) and (1.7) and derived the equation of states. In the limit $G$, $H^{\mu\nu} \rightarrow 0$, we have essentially recovered the results for $d>2$ reported by Kunz and Zumbach, but reached a different interpretation for the nature of the phase transition and the ordered state at $d \leq 2$. We have revealed that the occurrence of a phase transition in $d \leq 2$ dimensions is associated with the appearance of a bond long-range order, $\Delta_2 \sim |\langle \mathbf{S}_i \cdot \mathbf{S}_j \rangle| \neq 0$. As mentioned in Sec. V, the occurrence of such a symmetry breaking is a peculiarity of the $m \rightarrow \infty$ limit, since, for finite $m$, $\Delta_2$ is trivially zero at any temperature due to the underlying local symmetry of the system. In this sense, the $m \rightarrow \infty$ limit corresponds to a singular limit in this model. Thus, the interpretation by Kunz and Zumbach that the first-order transition found at $d=2$ is of topological origin mediated by vortex condensation is clearly inappropriate. It should be emphasized that the essentially same type of ordered state characterized by $\Delta_2 \neq 0$ persists even for two isolated spins which cannot sustain any topological object such as vortex.

The remaining part of this paper is organized as follows. We give exact solutions in one dimension in Sec. II. The case of an infinite-ranged interaction (mean-field theory) is treated in Sec. III. The high- and low-temperature series expansions are developed explicitly for general values of $m$ in Sec. IV. The large-$m$ limit of a short-range system is analyzed in Sec. V. Lastly Sec. VI is devoted to Summary and Discussions.

## II. EXACT SOLUTIONS IN $d=1$

The use of the transfer matrix method and the Funk-Hecke theorem[15] enables us to obtain an exact solution of the quadrupolar model (1.4) in one dimension. The treatment is quite similar to what treats the $m$-vector model (1.5). We first write the partition function as $Z=z^N$ and introduce the notation of spin traces:

$$\mathrm{Tr}=\prod_{i=1}^{N}\mathrm{Tr}_i\ ,\qquad \mathrm{Tr}_i[\,\cdots\,]=\frac{\int d\mathbf{S}_i\cdots\delta(S_0^2-\mathbf{S}_i^2)}{\int d\mathbf{S}_i\,\delta(S_0^2-\mathbf{S}_i^2)}\ . \tag{2.1}$$

Let us parallelly sketch the treatments for the $m$-vector model[16] and for the quadrupole model. The one-particle factor $z$ of the vector model is evaluated as

$$\begin{aligned}z_{\text{vector}}&=\mathrm{Tr}_i(e^{G\mathbf{S}_i\cdot\mathbf{S}_{i+1}/T})\\&=\frac{\int_{-1}^{1}e^{\alpha x}(1-x^2)^{(m-3)/2}dx}{\int_{-1}^{1}(1-x^2)^{(m-3)/2}dx}\\&={}_0F_1(m/2;\alpha^2/4)=1+\frac{\alpha^2}{2!}A_1+\frac{\alpha^4}{4!}A_2+\cdots\ ,\end{aligned} \tag{2.2}$$

where $\alpha=GS_0^2/T$ and ${}_0F_1(m/2;\alpha^4/4)$ is the generalized hypergeometric function[17] which may be rewritten as $\Gamma(m/2)(\alpha/2)^{1-m/2}I_{m/2-1}(\alpha)$. Here $I_\nu(x)$ and $\Gamma(x)$ denote, respectively, the modified Bessel function and the gamma function.[17] In an analogous way, the partition function of the quadrupolar model is given by $Z=z_{\text{quadrupole}}^N$ with

$$\begin{aligned}z_{\text{quadrupole}}&=\mathrm{Tr}_i[e^{J(\mathbf{S}_i\cdot\mathbf{S}_{i+1})^2/T}]\\&=\frac{\int_{-1}^{1}e^{\beta x^2}(1-x^2)^{(m-3)/2}dx}{\int_{-1}^{1}(1-x^2)^{(m-3)/2}dx}\\&={}_1F_1(\tfrac{1}{2};m/2;\beta)=1+\beta A_1+\frac{\beta^2}{2!}A_2+\cdots\ ,\end{aligned} \tag{2.3}$$

and the associated free energy $F$ reads

$$F/N=-T\ln z=-T\ln{}_1F_1(\tfrac{1}{2};m/2;\beta)\ , \tag{2.4}$$

where $\beta$ is the effective coupling $\beta=JS_0^4/T$ and ${}_1F_1(a;b;z)$ is the confluent geometric function.[17] In these two expansional equations (2.2) and (2.3) we put

$$A_1=\frac{1}{m},\quad A_2=\frac{3}{m(m+2)}\ ,\quad \ldots\ ,\quad A_k=\frac{\Gamma(m/2)\Gamma(\frac{1}{2}+k)}{\sqrt{\pi}\,\Gamma(m/2+k)}\ , \tag{2.5}$$

The internal energy $E$ can be obtained by evaluating the logarithmic derivatives with respect to $\alpha$ (or $\beta$):

$$-\frac{E}{NJS_0^2}=\frac{\partial}{\partial\alpha}\ln{}_0F_1(m/2;\alpha^2/4)=\frac{\alpha}{m}\,\frac{{}_0F_1((m+2)/2;\alpha^2/4)}{{}_0F_1(m/2;\alpha^2/4)} \tag{2.6a}$$

$$\begin{aligned}&=\frac{\partial}{\partial\alpha}\ln\left[1+\frac{\alpha^2}{2!}A_1+\frac{\alpha^4}{4!}A_2+\frac{\alpha^6}{6!}A_3+\cdots\right]\\&=\alpha A_1+\alpha^3\left[\frac{A_2}{2!}-\frac{A_1^2}{2}\right]+\alpha^5\left[\frac{A_3}{5!}-\frac{A_1A_2}{8}+\frac{A_1^3}{4}\right]+\cdots\\&=\frac{\alpha}{m}+\left[\frac{\alpha}{m}\right]^3Q_1+\left[\frac{\alpha}{m}\right]^5Q_2+\left[\frac{\alpha}{m}\right]^7Q_3+\left[\frac{\alpha}{m}\right]^9Q_4+\cdots\end{aligned} \tag{2.6b}$$

for the vector model and

$$-\frac{E}{NJS_0^4}=\frac{\partial}{\partial\beta}\ln{}_1F_1(\tfrac{1}{2};m/2;\beta)=1+\frac{m-1}{2\beta}\left[\frac{{}_1F_1(-\frac{1}{2};m/2;\beta)}{{}_1F_1(\frac{1}{2};m/2;\beta)}-1\right] \tag{2.7a}$$

$$\begin{aligned}&=\frac{\partial}{\partial\beta}\ln\left[1+\beta A_1+\frac{\beta^2}{2!}A_2+\frac{\beta^3}{3!}A_3+\cdots\right]\\&=A_1+\beta(A_2-A_1^2)+\beta^2\left[\frac{A_3}{2}-\frac{3}{2}A_1A_2+A_1^3\right]+\cdots\\&=\frac{R_{-1}}{m}\left[R_0+\frac{2\beta}{m}R_1+\left[\frac{2\beta}{m}\right]^2R_2+\left[\frac{2\beta}{m}\right]^3R_3+\left[\frac{2\beta}{m}\right]^4R_4+\left[\frac{2\beta}{m}\right]^5R_5+\cdots\right]\end{aligned} \tag{2.7b}$$

for the quadrupolar model. The explicit $m$-dependent forms for the spin-trace functions $Q_1, Q_2, \ldots$ and $R_{-1}, R_0, R_1, \ldots$ are listed in Table I. These expansional expressions (2.6b) and (2.7b) offer the high-temperature series in a one-dimensional lattice, which will be useful in a later analysis in higher dimensions (see Sec. IV A for the quadrupolar model). However, there is no phase transition in this one-dimensional system except for $m=\infty$. Let us briefly consider this $m \to \infty$ limit. Putting

$$K=\frac{\beta}{m}=\frac{JS_0^4}{mT} \tag{2.8}$$

and taking the limit $m \to \infty$ in (2.7a) we find

$$\begin{aligned} -\frac{E}{NJS_0^4} &= 1+\frac{1}{2K}\left[\frac{{}_1F_1(-\frac{1}{2};m/2;mK)}{{}_1F_1(\frac{1}{2};m/2;mK)}-1\right] \\ &= \begin{cases} O(1/m), & \text{for } K<\frac{1}{2} \\ 1-\dfrac{1}{2K}+O(1/m), & \text{for } K>\frac{1}{2}\,. \end{cases} \end{aligned} \tag{2.9}$$

Thus a second-order phase transition occurs at $K_c = JS_0^4/mT_c = \frac{1}{2}$ for $m=\infty$ and $d=1$. The same result (2.9) will be rederived from the independent analysis in the large-$m$ limit in Sec. V; see (5.19a).

## III. EXACT SOLUTION OF AN INFINITE-RANGE SYSTEM: MEAN-FIELD THEORY

The Hamiltonian of a generalized quadrupolar model with an infinite-ranged interaction and a field is given by

$$\mathcal{H}=-\frac{J}{2N}\sum_{i,j=1}^{N}\sum_{\mu,\nu=1}^{m}\phi_i^{\mu\nu}\phi_j^{\mu\nu}-\sum_{i=1}^{N}\sum_{\mu,\nu=1}^{m}H^{\mu\nu}\phi_i^{\mu\nu}\,. \tag{3.1}$$

Here $\phi_i^{\mu\nu}$ is a *symmetric traceless tensor* which has vanishing mean at infinite temperature:

$$\langle \phi_i^{\mu\nu}\rangle = 0 \quad \text{at } T=\infty\,. \tag{3.2}$$

In the case of the uniaxial quadrupoles introduced in Sec. I, $\phi_i^{\mu\nu}=S_i^{\mu}S_i^{\nu}-S_0^2\delta_{\mu\nu}/m$ is taken for granted. In this case, the field term in (3.1) becomes identical to (1.7). In (3.1) the sum $ij$ runs over all quadrupole pairs, including the term with $i=j$ also. It is only because of the infinite range of the interactions that the $i=j$ term does not matter.

The free energy of this system reads

$$F=-T\ln \mathrm{Tr}\left[\prod_{\mu,\nu=1}^{m}\exp\left[\frac{J}{2NT}\sum_{i,j=1}^{N}\phi_i^{\mu\nu}\phi_j^{\mu\nu}+\frac{H^{\mu\nu}}{T}\sum_{i=1}^{N}\phi_i^{\mu\nu}\right]\right], \tag{3.3}$$

where $\mathrm{Tr}=\prod_{i=1}^{N}\mathrm{Tr}_i$ denotes the phase-space integral for all quadrupoles introduced in (2.1). This free energy can be evaluated as follows. First we rewrite the summation over particles as a quadrate in the first term in the exponential and get

TABLE I. The spin-trace functions appearing in the high-temperature series in the one-dimensional systems. $Q_1, Q_2, \ldots$ appear in the vector model and $R_{-1}, R_0, R_1, \ldots$ appear in the quadrupolar model.

$$Q_1=-\frac{m}{m+2}, \qquad Q_2=\frac{2m^2}{(m+2)(m+4)}\,,$$

$$Q_3=-\frac{m^3(5m+12)}{(m+2)^2(m+4)(m+6)}, \qquad Q_4=\frac{2m^4(7m+24)}{(m+2)^2(m+4)(m+6)(m+8)}\,,$$

---

$$R_{-1}=\frac{m-1}{m+2}, \qquad R_0=\frac{1}{R_{-,}}=\frac{m+2}{m-1}, \qquad R_1=1, \qquad R_2=\frac{m-2}{m+4}\,,$$

$$R_3=\frac{(m-4)(m^2+m-3)}{(m+2)(m+4)(m+6)}, \qquad R_4=\frac{(m-2)(m^3-5m-17m+24)}{(m+2)(m+4)(m+6)(m+8)}\,,$$

$$R_5=\frac{m^7-6m^6-66m^5+78m^4+798m^3-552m^2-2128m+1920}{(m+2)^2(m+4)^2(m+6)(m+8)(m+10)}\,,$$

$$R_6=\frac{(m-2)(m^7-10m^6-110m^5+182m^4+2278m^3-712m^2-7344m+5760)}{(m+2)^2(m+4)^2(m+6)(m+8)(m+10)(m+12)}\,,$$

$$R_7=\frac{m^{11}-11m^{10}-251m^9-21m^8+11487m^7+21483m^6-154717m^5-204874m^4+859592m^3+229728m^2-1729152m+967680}{(m+2)^3(m+4)^2(m+6)^2(m+8)(m+10)(m+12)(m+14)}\,.$$

$$F=-T\ln\mathrm{Tr}\left\{\prod_{\mu,\nu=1}^{m}\exp\left[\frac{J}{2NT}\left[\sum_{i}^{N}\phi_i^{\mu\nu}\right]^2+\frac{H^{\mu\nu}}{T}\sum_{i}^{N}\phi_i^{\mu\nu}\right]\right\}. \tag{3.4}$$

Second, putting $a^{\mu\nu}=\sqrt{J/NT}\,\sum_i^N\phi_i^{\mu\nu}$ we apply the identity

$$\exp\left[\frac{(a^{\mu\nu})^2}{2}\right]=\frac{1}{\sqrt{2\pi}}\int_{-\infty}^{\infty}\exp\left[-\frac{(\zeta^{\mu\nu})^2}{2}+\zeta^{\mu\nu}a^{\mu\nu}\right]d\zeta^{\mu\nu} \tag{3.5}$$

$m^2$ times to introduce an integral representation for the free energy:

$$\begin{aligned}F&=-T\ln\mathrm{Tr}\left\{\prod_{\mu,\nu=1}^{m}\int_{-\infty}^{\infty}d\zeta^{\mu\nu}\exp\left[-\frac{(\zeta^{\mu\nu})^2}{2}\right]\exp\left[\zeta^{\mu\nu}\left[\frac{J}{NT}\right]^{1/2}\sum_{i}^{N}\phi_i^{\mu\nu}+\frac{H^{\mu\nu}}{T}\sum_{i}^{N}\phi_i^{\mu\nu}\right]\right\}\\&=-T\ln\left[\int_{-\infty}^{\infty}\left[\prod_{\mu,\nu=1}^{m}d\zeta^{\mu\nu}\right]\exp\left[-\sum_{\mu,\nu=1}^{m}\frac{(\zeta^{\mu\nu})^2}{2}\right]\left[\mathrm{Tr}_1\exp\left\{\sum_{\mu,\nu=1}^{m}\left[\zeta^{\mu\nu}\left[\frac{J}{NT}\right]^{1/2}+\frac{H^{\mu\nu}}{T}\right]\phi_1^{\mu\nu}\right\}\right]^N\right].\end{aligned} \tag{3.6}$$

The factor $1/\sqrt{2\pi}$ is irrelevant in the potential $F$ and has been dropped. Now we may utilize the method of steepest descent because only the maximal value of the integrand contributes in the limit $N\to\infty$. Thus the actual free energy is given by its minimum with respect to $\zeta^{\mu\nu}$:

$$F=-T\min_{\zeta^{\mu\nu}}\ln\left[\exp\left[-\sum_{\mu,\nu=1}^{m}\frac{(\zeta^{\mu\nu})^2}{2}\right]\left[\mathrm{Tr}_1\exp\left\{\sum_{\mu,\nu=1}^{m}\left[\zeta^{\mu\nu}\left[\frac{J}{NT}\right]^{1/2}+\frac{H^{\mu\nu}}{T}\right]\phi_1^{\mu\nu}\right\}\right]^N\right]. \tag{3.7}$$

Substituting $y^{\mu\nu}=\zeta^{\mu\nu}\sqrt{T/NJ}$ in (3.7) we obtain as the normalized free energy per one particle

$$\frac{F}{NT}=\min_{y^{\mu\nu}}\{f(y^{\mu\nu})\}, \tag{3.8a}$$

where

$$f(y^{\mu\nu})=\frac{J}{T}\sum_{\mu,\nu=1}^{m}\frac{(y^{\mu\nu})^2}{2}-\ln\mathrm{Tr}_1\left[\exp\left[\sum_{\mu,\nu=1}^{m}\frac{1}{T}(Jy^{\mu\nu}+H^{\mu\nu})\phi_1^{\mu\nu}\right]\right]. \tag{3.8b}$$

At this moment, applying the minimal conditions $\partial f/\partial y^{\alpha\beta}=0$ leads us to $m^2$ necessary conditions for a minimum in $m^2$ space, namely,

$$y^{\alpha\beta}=\langle\phi_1^{\alpha\beta}\rangle=\frac{\mathrm{Tr}_1\left[\phi_1^{\alpha\beta}\exp\left[\sum_{\mu,\nu=1}^{m}\frac{1}{T}(Jy^{\mu\nu}+H^{\mu\nu})\phi_1^{\mu\nu}\right]\right]}{\mathrm{Tr}_1\left[\exp\left[\sum_{\mu,\nu=1}^{m}\frac{1}{T}(Jy^{\mu\nu}+H^{\mu\nu})\phi_1^{\mu\nu}\right]\right]}, \tag{3.9}$$

This equation indicates that $y^{\alpha\beta}$ is an ensemble average of $\phi_1^{\alpha\beta}$. The set of extremum parameters, $y^{\mu\nu}$, thus are identified as a tensor order parameter of this system. Note that the right-hand side of (3.9) is just the usual definition of the order parameter against the field $H^{\alpha\beta}$; one can rederive (3.9) from a relation $y^{\alpha\beta}=-\partial f/\partial H^{\alpha\beta}$. Now it is easy to see that this tensor order parameter is traceless because $\phi_1^{\mu\nu}$ itself is traceless. Moreover, differentiating (3.8) with respect to $1/T$, we find that the internal energy $E$ per one particle is given by

$$\frac{E}{N}=\frac{\partial f}{\partial(1/T)}=-J\sum_{\mu,\nu=1}^{m}\frac{(y^{\mu\nu})^2}{2}-\sum_{\mu,\nu=1}^{m}H^{\mu\nu}y^{\mu\nu}. \tag{3.10}$$

In the discussion below we restrict ourselves to the case of the uniaxial quadrupoles and set all fields $H^{\mu\nu}$ equal to zero. The order parameter $y^{\mu\nu}$ in this case is then identical to the usual quadrupolar order parameter (1.6). Moreover we do not try to find all local minima of $f(y^{\mu\nu})$ in $m^2$ space, but we investigate all tensors $y^{\mu\nu}$ with only nonzero diagonal elements. Let us assume $y^{\alpha\beta}\equiv0$ in the high-temperature side ($T>T_c$) and

$$y^{\alpha\beta}=\Delta S_0^2\left[\delta_{\alpha1}\delta_{\beta1}-\frac{\delta_{\alpha\beta}}{m}\right] \tag{3.11}$$

in the low-temperature side ($T<T_c$). The choice of this order parameter $\Delta$ corresponds to an ordered state where the director points to the first axis in spin space. From (3.8) we obtain

$$f=0,\quad\text{for } T>T_c \tag{3.12a}$$

$$\begin{aligned}&=(m-1)\frac{J\Delta^2S_0^4}{2mT}+x-\ln{}_1F_1(\tfrac{1}{2};m/2;mx)\\&=\frac{m-1}{2}x\Delta-\frac{R_{-1}}{2}\sum_{l=1}^{\infty}\frac{R_l}{l+1}(2x)^{l+1},\quad\text{for}T<T_c,\end{aligned} \tag{3.12b}$$

where $R_l$ is the functions given in Table I and $x$ is a new parameter defined by

$$x=K\Delta=\frac{JS_0^4\Delta}{mT}. \tag{3.13}$$

By expanding (3.12b) around $\Delta=0$ we obtain the spinodal point $K_{\mathrm{sp}}=(m+2)/2$. When $K=K_{\mathrm{sp}}$, disordered states become unstable with respect to infinitesimal perturbations. The explicit derivation of (3.12) is relegated to Appendix A. On the low-temperature side we should impose the extremum condition (3.8a) with respect to the order parameter $\Delta$,

$$\Delta\frac{\partial f}{\partial \Delta}=(m-1)\left[\frac{JS_0^4\Delta^2}{mT}-x\right]-\frac{m-1}{2}\left[\frac{{}_1F_1(-\frac{1}{2};m/2;mx)}{{}_1F_1(\frac{1}{2};m/2;mx)}-1\right]=0\ . \qquad (3.14)$$

Then to use (3.14) in (3.12) yields

$$\frac{F(x)}{NT}=\frac{m+1}{2}x+\frac{m-1}{4}\left[\frac{{}_1F_1(-\frac{1}{2};m/2;mx)}{{}_1F_1(\frac{1}{2};m/2;mx)}-1\right]-\ln {}_1F_1(\tfrac{1}{2};m/2;mx)\ , \qquad (3.15)$$

which is a function of only $x$ defined by (3.13). The curve $F(x)/NT$ is shown for several values of $m$ in Fig 2. There is a phase transition at $x=x_c$ where $F(x_c)=0$. The order parameter $\Delta$ is related to the variable $x$ through the equation

$$\Delta=1+\frac{1}{2x}\left[\frac{{}_1F_1(-\frac{1}{2};m/2;mx)}{{}_1F_1(\frac{1}{2};m/2;mx)}-1\right]\ , \qquad (3.16)$$

which is obviously derived from Eqs. (3.13) and (3.14). It is interesting to note that the same function as in (3.16) appears in the exact solution in one dimension except that the argument differs by a factor $\Delta$ [compare (2.7a) with (3.16)]. Figure 3 shows the $x$ dependence of the order parameter $\Delta$ given by (3.16). On the other hand, from (3.10) one finds that the internal energy is related to the order parameter $\Delta$ via

$$\frac{E}{NJS_0^4}=-\frac{m-1}{2m}\Delta^2\ , \qquad (3.17)$$

i.e., the internal energy is simply proportional to the square of the order parameter.

For $m=2$, the system undergoes a second-order phase transition because $F(x)$ is always negative for all $x>0$ and therefore $x_c=0$. For general values of $m$, however, the transition is first order as is expected. The transition point $x_c$ (and $K_c=JS_0^4/mT_c$) and the discontinuities of the order parameter $\Delta_c$ and of the internal energy $\Delta E_c$ are listed in Table II for various values of $m$.

The investigation of the $m\to\infty$ limit in this infinite-range system helps us to understand the present analysis more distinctly, because all the relevant functions become elementary. First, taking the limit $m\to\infty$ in (3.16) gives

$$\Delta=\begin{cases} O\left[\dfrac{1}{m}\right] & \text{for } x<\frac{1}{2} \\ 1-\dfrac{1}{2x}+O\left[\dfrac{1}{m}\right] & \text{for } x>\frac{1}{2} \end{cases}$$

[rigorously same procedure as in (2.9)]. Substituting this result for $x>\frac{1}{2}$ into (3.13) we get

$$x=\tfrac{1}{2}[K+\sqrt{K(K-2)}]\quad\text{or}\quad K=\frac{2x^2}{2x-1} \qquad (3.18)$$

with $K=JS_0^4/mT$. Obviously the solution for the low-temperature phase, (3.12b), does not exist for $x<1$ (i.e., $K<2$) because $x$ becomes pure imaginary in this region. The point at which the ordered state becomes unstable with respect to infinitesimal perturbations has been denoted by second spinodal[18] or $K_{\mathrm{sp}2}$; therefore this value is $K_{\mathrm{sp}2}=2$ in the large-$m$ limit. Equation (3.15) becomes

$$\frac{F(x)}{NT}=\frac{m}{2}\left[-x+\frac{1}{2}+\ln(2x)+O\left[\frac{1}{m}\right]\right] \qquad (3.19)$$

and the transition point determined by the condition $F(x_c)=0$ is

$$x_c=1.756\,43\quad(K_c=2.4554)\ , \qquad (3.20)$$

below which the low-temperature phase becomes *metastable*. Thus we should have

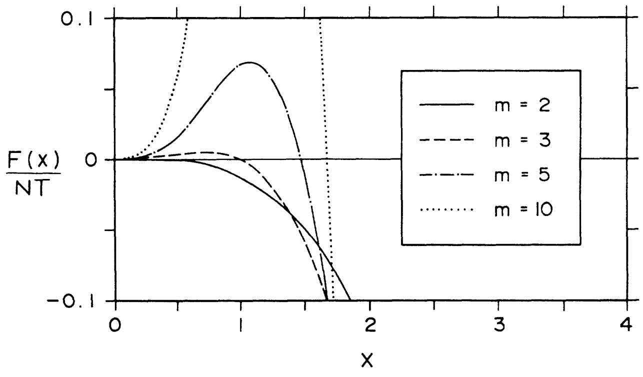

FIG. 2. Free energy in the low-temperature phase, (3.15), as a function of $x=J\Delta S_0^4/mT$ for $m=2$, 3, 5, and 10. The transition point $x_c$ is determined as the crossing of this curve and the $x$ axis corresponding to the free energy in the high-temperature phase.

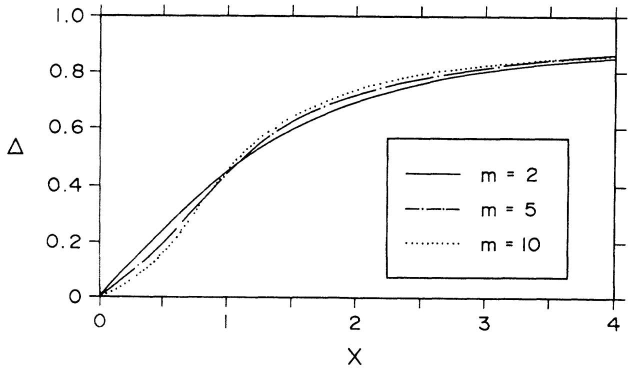

FIG. 3. The order parameter $\Delta$ in the low-temperature side ($x>x_c$) given by (3.16). Three curves are corresponding, respectively, to $m=2$, 5, and 10. This $\Delta$ is constantly zero in the high-temperature side ($x<x_c$) and abruptly jumps to finite $\Delta_c$ at the transition point.

TABLE II. The numerical values of the transition point $x_c$, $K_c$, the order-parameter jump $\Delta_c$, and the energy jump $\Delta E_c$ of the infinite-range system for various $m$.

| | | | | |
|---|---|---|---|---|
| $m=1$ | | $f\equiv 0$, since "up" is equivalent to "down" | | |
| $m=2$ | $x_c=0.00$ | $K_c=2.00$ | $\Delta_c=0.00$ | $\Delta E_c/NJS_0^4=0.00$ |
| $m=3$ | $x_c=0.97$ | $K_c=2.27$ | $\Delta_c=0.43$ | $\Delta E_c/NJS_0^4=0.06$ |
| $m=4$ | $x_c=1.31$ | $K_c=2.34$ | $\Delta_c=0.56$ | $\Delta E_c/NJS_0^4=0.12$ |
| $m=5$ | $x_c=1.47$ | $K_c=2.40$ | $\Delta_c=0.61$ | $\Delta E_c/NJS_0^4=0.15$ |
| $m=6$ | $x_c=1.56$ | $K_c=2.42$ | $\Delta_c=0.64$ | $\Delta E_c/NJS_0^4=0.17$ |
| $m=7$ | $x_c=1.61$ | $K_c=2.43$ | $\Delta_c=0.66$ | $\Delta E_c/NJS_0^4=0.19$ |
| $m=8$ | $x_c=1.63$ | $K_c=2.44$ | $\Delta_c=0.67$ | $\Delta E_c/NJS_0^4=0.20$ |
| $m=9$ | $x_c=1.66$ | $K_c=2.44$ | $\Delta_c=0.68$ | $\Delta E_c/NJS_0^4=0.21$ |
| $m=10$ | $x_c=1.68$ | $K_c=2.44$ | $\Delta_c=0.69$ | $\Delta E_c/NJS_0^4=0.21$ |
| $m=20$ | $x_c=1.73$ | $K_c=2.45$ | $\Delta_c=0.70$ | $\Delta E_c/NJS_0^4=0.23$ |
| $m=30$ | $x_c=1.74$ | $K_c=2.45$ | $\Delta_c=0.71$ | $\Delta E_c/NJS_0^4=0.24$ |
| $m=40$ | $x_c=1.74$ | $K_c=2.45$ | $\Delta_c=0.71$ | $\Delta E_c/NJS_0^4=0.25$ |
| $m=50$ | $x_c=1.75$ | $K_c=2.45$ | $\Delta_c=0.71$ | $\Delta E_c/NJS_0^4=0.25$ |
| $m=\infty$ | $x_c=1.7564$ | $K_c=2.4554$ | $\Delta_c=0.7153$ | $\Delta E_c/NJS_0^4=0.2528$ |

$$\Delta=\begin{cases}0, & \text{for } x<x_c\\ 1-\dfrac{1}{2x} & \text{for } x>x_c\end{cases} \tag{3.21}$$

for thermal equilibrium. From (3.20) and (3.21) the discontinuity in the order parameter at the transition point is evaluated as

$$\Delta_c=1-\frac{1}{2x_c}=0.715\,332 \tag{3.22}$$

and the resulting $K$-$\Delta$ curve is shown in Fig. 4 together with the spinodal point $K_{\mathrm{sp}}=\infty$ and the second spinodal point $K_{\mathrm{sp2}}=2$ for the $m\to\infty$ limit. In the same figure, the $K$-$\Delta$ curve for $m=3$ and a typical value for the critical order parameter $\Delta_c$ of liquid crystals[19] are also shown for comparison. From these curves, the temperature-dependence of the internal energy $E$ is readily obtained via Eq. (3.17).

Before ending this section we make a comment on expansional expressions of the free energy. In (3.8) we could expand the free energy with respect to the order parameter up to a finite order. The result up to the fourth order is given by

$$\begin{aligned}f={}&\frac{J}{T}\sum_{\mu,\nu=1}^{m}\frac{(y^{\mu\nu})^2}{2}-\frac{J^2}{2T^2}\mathrm{Tr}_1\left[\sum_{\mu,\nu=1}^{m}z^{\mu\nu}\phi_1^{\mu\nu}\right]^2-\frac{J^3}{6T^3}\mathrm{Tr}_1\left[\sum_{\mu,\nu=1}^{m}z^{\mu\nu}\phi_1^{\mu\nu}\right]^3\\&+\frac{J^4}{T^4}\left\{-\frac{1}{24}\mathrm{Tr}_1\left[\sum_{\mu,\nu=1}^{m}z^{\mu\nu}\phi_1^{\mu\nu}\right]^4+\frac{1}{8}\left[\mathrm{Tr}_1\left[\sum_{\mu,\nu=1}^{m}z^{\mu\nu}\phi_1^{\mu\nu}\right]^2\right]^2\right\}\\={}&\frac{J}{T}\sum_{\mu,\nu=1}^{m}\frac{(y^{\mu\nu})^2}{2}-\frac{J^2}{2T^2}\sum_{\mu,\nu,\alpha,\beta=1}^{m}z^{\mu\nu}z^{\alpha\beta}\mathrm{Tr}_1[\phi_1^{\mu\nu}\phi_1^{\alpha\beta}]-\frac{J^3}{6T^3}\sum_{\mu,\nu,\alpha,\beta,\gamma,\epsilon=1}^{m}z^{\mu\nu}z^{\alpha\beta}z^{\gamma\epsilon}\mathrm{Tr}_1[\phi_1^{\mu\nu}\phi_1^{\alpha\beta}\phi_1^{\gamma\epsilon}]\\&+\frac{J^4}{T^4}\sum_{\mu,\nu,\alpha,\beta,\gamma,\epsilon,\rho,\sigma=1}^{m}z^{\mu\nu}z^{\alpha\beta}z^{\gamma\epsilon}z^{\rho\sigma}\left(-\tfrac{1}{24}\mathrm{Tr}_1[\phi_1^{\mu\nu}\phi_1^{\alpha\beta}\phi_1^{\gamma\epsilon}\phi_1^{\rho\sigma}]+\tfrac{1}{8}\mathrm{Tr}_1[\phi_1^{\mu\nu}\phi_1^{\alpha\beta}]\mathrm{Tr}_1[\phi_1^{\gamma\epsilon}\phi_1^{\rho\sigma}]\right),\end{aligned} \tag{3.23}$$

where we put $z^{\mu\nu}=y^{\mu\nu}+H^{\mu\nu}/J$. A somewhat more restricted form of the free energy expansion has been proposed only from symmetry considerations by de Gennes[8] and Lubensky and Priest,[9] which might be applicable in the isotropic (high-temperature) phase. For uniaxial quadrupoles the explicit coefficients are now obtained from (3.23) not only in the isotropic phase but also in the anisotropic (low-temperature) phase, by using the relation

$$\mathrm{Tr}_1[S_1^{(1)}]^{2l_1}[S_1^{(2)}]^{2l_2}\cdots[S_1^{(k)}]^{2l_k}=S_0^{2L}\frac{(m-2)!!\,(2l_1-1)!!\,(2l_2-1)!!\,\cdots\,(2l_k-1)!!}{[m+2(L-1)]!!}, \tag{3.24}$$

with $L=l_1+l_2+\cdots+l_k$, $(2l-1)!!=(2l-1)(2l-3)\times\cdots 3\times 1$, and $(2l)!!=(2l)(2l-2)\times\cdots\times 2$. The derivation of this relation is given in Appendix B. Evaluating the expansional coefficients in (3.23) by applying (3.24) we find following three facts to be exaggerated. First, for $m\geq 4$, this free energy expansion up to the fourth order fails because the coefficient at the fourth order becomes negative for the ordinary choice of the order parameter (3.10). An easier check of this fact is to utilize the expansional form of (3.12b); the function $-R_{-1}R_3$ is positive only for $(\sqrt{13}-1)/2<m<4$. Second, if the term proportional to $J^3$ (the third order term) vanishes, the transition into the ordered phase is of second order. One may easily check that this term vanishes actually for $m=2$. Third, we could alternatively consider the nondiagonal case of the order parameter, e.g.,

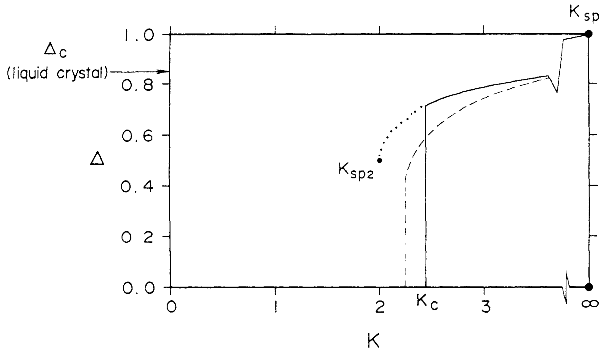

FIG. 4. The $K$ dependence of the order parameter $\Delta$ of the infinite-range system. The straight and dotted lines indicate the large-$m$ limit and the corresponding exact expression is given by (3.21) with (3.18). The broken line indicates the case of $m=3$. A typical value for the critical order parameter, $\Delta_c$, for a liquid crystal (Ref. 19) is included (marked with an arrow) for comparison.

$$y^{\alpha\beta}=\Delta S_0^2(\delta_{\alpha 1}\delta_{\beta 2}+\delta_{\alpha 2}\delta_{\beta 1}) \tag{3.25}$$

instead of (3.11). From an analogous computation we estimated the instability point $K_{\text{inst}}$ against the nondiagonal order described by (3.25). Because this $K_{\text{inst}}$ is large compared to the $K_c$ evaluated by using (3.11) we conclude that such an order does not emerge in equilibrium.

## IV. SERIES ANALYSIS

### A. High-temperature series

The high-temperature series expansion for the $m$-component quadrupolar model (1.4) can be developed along the same line as that for the $m$-vector model (1.5) which has been treated by Stanley and Kaplan,[20] Stanley,[21] and Ohno, Okabe, and Morita.[22] Consider the internal energy or the ($fg$-bond) correlation function defined by

$$G(f,g)=\frac{\mathrm{Tr}[(\mathbf{S}_f\cdot\mathbf{S}_g)^2 e^{-\mathcal{H}/T}]}{\mathrm{Tr}[e^{-\mathcal{H}/T}]} . \tag{4.1}$$

Here the Hamiltonian $\mathcal{H}$ and the spin trace Tr are defined, respectively, in (1.4) and (2.1). Using the graphical expansion by drawing each interaction $\mathcal{H}_{ij}=-J_{ij}(\mathbf{S}_i\cdot\mathbf{S}_j)^2$ with a straight line and expanding (4.1) in a power series of $2K=2JS_0^4/mT$, we formally have

$$G(f,g)=\sum_{l=0}^{\infty}(2K)^l\sum_{\mathcal{D}_{fg}}\alpha_l(\mathcal{D}_{fg})\rho_l(\mathcal{D}_{fg}) , \tag{4.2}$$

where $\alpha_l(\mathcal{D}_{fg})$ denotes the weight function of one $l$th order graph $\mathcal{D}_{fg}$, which stems from just the spin traces, and $\rho_l(\mathcal{D}_{fg})$ is the number of its realization on the assumed lattice. The notation $\mathcal{D}_{fg}$ denotes the graph which is made from the $(l+1)$th order graph $\mathcal{D}$ by changing one interaction line on $fg$-bond into one external line $(\mathbf{S}_f\cdot\mathbf{S}_g)^2$ appearing in the numerator of (4.1). It is convenient to draw this external line by a wavy line, while we draw all the other interaction lines by straight lines; see Fig. 5(a), for example. Now writing

$$\begin{gathered}\mathrm{Tr}\left[(\mathbf{S}_f\cdot\mathbf{S}_g)^2\left[\frac{-\mathcal{H}}{T}\right]^l\right]=(2K)^l\sum_{\mathcal{D}_{fg}}\nu_l(\mathcal{D}_{fg})\rho_l(\mathcal{D}_{fg}) ,\\ \mathrm{Tr}\left[\left[\frac{-\mathcal{H}}{T}\right]^l\right]=(2K)^l\sum_{\mathcal{D}}\mu_l(\mathcal{D})\rho_l(\mathcal{D}) ,\end{gathered} \tag{4.3}$$

we derive

$$\alpha_l(\mathcal{D}_{fg})=\nu_l(\mathcal{D}_{fg})-\sum_{k=0}^{l-1}\sum_{\mathcal{D}'_{fg}+\mathcal{D}''=\mathcal{D}_{fg}}\alpha_k(\mathcal{D}'_{fg})\mu_{l-k}(\mathcal{D}'') \tag{4.4}$$

from (4.1), where the condition $\mathcal{D}'_{fg}+\mathcal{D}''=\mathcal{D}_{fg}$ indicates that this summation runs over all possible ways in decomposing the graph $\mathcal{D}_{fg}$ into two subgraphs $\mathcal{D}'_{fg}$ and $\mathcal{D}''$. It is, however, not necessary to include in $\mathcal{D}_{fg}$ or $\mathcal{D}'_{fg}$ any unlinked graphs or any graphs involving at least one articulation point. (If the graph splits into two disconnected parts by cutting at one point, we call this point the articulation point.) That $\alpha_l$ of such a graph disappears is indeed derived from (4.4) in the case of the quadrupolar model as well as the vector model. It is a matter of simple algebra to evaluate the spin traces $\nu_l(\mathcal{D}'_{fg})$ and $\mu_l(\mathcal{D}'')$ by means of the mathematical formula (3.24). Then the weight function $\alpha_l(\mathcal{D}_{fg})$ can be evaluated order by order through (4.4) using the spin trace functions and the $\alpha_k$ for lower order graphs.

It is important to notice that the weight functions $\alpha_l(\mathcal{D}_{fg})$ of topologically distinct graphs are not always independent. To see this we consider the expansion coefficients of the free energy defined as

$$\ln\mathrm{Tr}[e^{-\mathcal{H}/T}]=\frac{m}{2S_0^4}\sum_{l=1}^{\infty}(2K)^l\sum_{\mathcal{D}}\lambda_l(\mathcal{D})\rho_l(\mathcal{D}) . \tag{4.5}$$

Then the weight function $\lambda_{l+1}(\mathcal{D})$ is related to $\alpha_l(\mathcal{D}_{fg})$ via the relation

$$\alpha_l(\mathcal{D}_{fg})=l_{fg}\lambda_{l+1}(\mathcal{D})\ \text{(theorem 1)} , \tag{4.6}$$

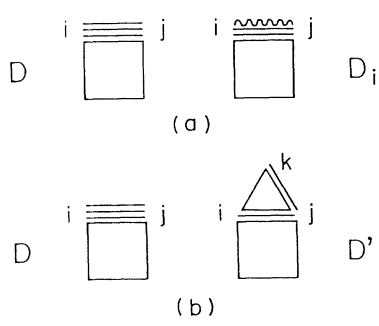

FIG. 5. Illustration of the two theorems (4.6) and (4.7). Theorem 1 represents the relation between the free energy diagram $\mathcal{D}$ and the susceptibility (or energy) diagram $\mathcal{D}_{ij}$ which are shown in (a). Theorem 2 represents the relation between two free energy diagrams $\mathcal{D}$ and $\mathcal{D}'$ as in (b).

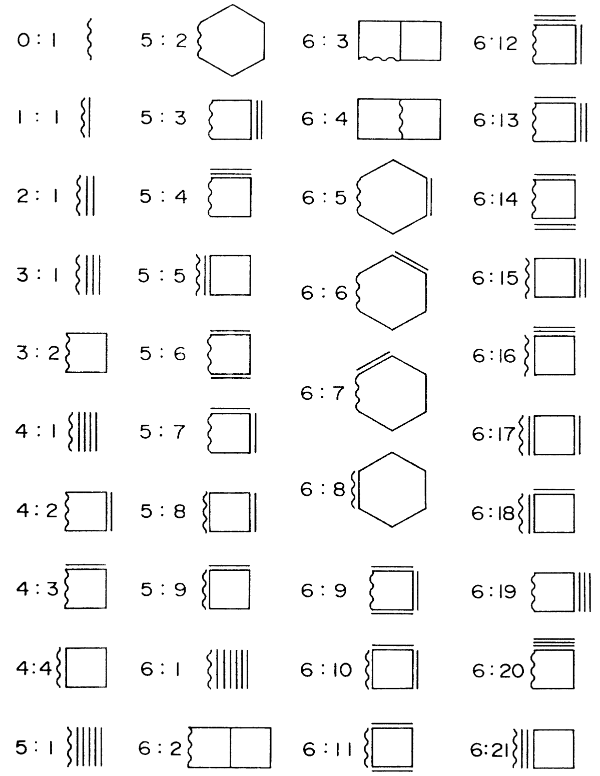

FIG. 6. The energy diagrams appearing up to the sixth order. Each contribution is tabulated in Table III.

where $l_{fg}$ denotes the number of interaction lines on $fg$-bond of the graph $\mathcal{D}$. The relation between the graphs $\mathcal{D}_{fg}$ and $\mathcal{D}$ is the same as above; see Fig. 5(a) also. The $\lambda$'s for many kinds of graphs are indeed not mutually independent. Let us consider the graph $\mathcal{D}$ which has $l_{ij}$ interaction lines on $ij$-bond. If we move one of these interaction lines onto $ik$-bond ($k$ is the new point which connected no interaction lines before) and newly add $l_{kj}$ interaction lines on $kj$-bond as is illustrated in Fig. 5(b), then the weight of the corresponding graph $\mathcal{D}'$ is given by

$$\lambda_{l+l_{kj}+1}(\mathcal{D}')=l_{ij}qR_{l_{kj}}\lambda_l(\mathcal{D}) \quad \text{(theorem 2)} , \tag{4.7}$$

where

$$q=\frac{1}{m+2} \tag{4.8}$$

and $R_k$ is the same function appearing in the coefficients in the case of the one-dimensional lattice; explicit forms of $R$'s are listed in Table I. The proofs of theorems 1 and 2 are given in Appendix C.

The graphs appearing in the expansion of the internal energy can be evaluated by using (4.4) or by using these theorems. All the graphs needed in considering to the sixth order in the square and cubic lattices are presented in Fig. 6 and the corresponding weight functions $m\alpha_l(\mathcal{D}_{fg})/R_{-1}S_0^4$ and realization numbers $\rho_l(\mathcal{D}_{fg})$ are listed in Table III. It is more labor saving to list up all weight functions $\lambda$'s rather than $\alpha$'s. The graphs appearing in the free energy up to the seventh order are shown in Fig. 7 together with the weight functions $m\lambda_l(\mathcal{D})/R_{-1}S_0^4$. The graphs appearing at the eighth order are in Fig. 8. The explicit form of the spin-trace functions $R_i$ are already given in Table I and the other functions $W_i$ are listed in Table IV. The series for the internal energy $E$ up to order $K^7$ can thus be evaluated for general component number $m$. In the case of the simple cubic lattice, the result is given by

TABLE III. The weight function $m\alpha_l(\mathcal{D}_{fg})/R_{-1}S_0^4$ and the realization number $\rho_l(\mathcal{D})$ relevant to the energy up to order $K^6$ for the square (sq.) and simple cubic (c.) lattices.

| No. | Weight | sq. | c. | No. | Weight | sq. | c. |
|---|---|---|---|---|---|---|---|
| 0:1 | $R_0$ | 1 | 1 | 6:3 | $2R_2q^4$ | 4 | 24 |
| 1:1 | $R_1=1$ | 1 | 1 | 6:4 | $2R_2q^4$ | 1 | 6 |
| 2:1 | $R_2$ | 1 | 1 | 6:5 | $R_2q^4$ | 6 | 44 |
| 3:1 | $R_3$ | 1 | 1 | 6:6 | $R_2q^4$ | 12 | 88 |
| 3:2 | $q^2$ | 2 | 4 | 6:7 | $R_2q^4$ | 12 | 88 |
| 4:1 | $R_4$ | 1 | 1 | 6:8 | $2R_2q^4$ | 6 | 44 |
| 4:2 | $R_2q^2$ | 2 | 4 | 6:9 | $R_2^3q^2$ | 2 | 4 |
| 4:3 | $R_2q^2$ | 4 | 8 | 6:10 | $2R_2^3q^2$ | 4 | 8 |
| 4:4 | $2R_2q^2$ | 2 | 4 | 6:11 | $2R_2^3q^2$ | 2 | 4 |
| 5:1 | $R_5$ | 1 | 1 | 6:12 | $R_2R_3q^2$ | 4 | 8 |
| 5:2 | $q^4$ | 6 | 44 | 6:13 | $R_2R_3q^2$ | 4 | 8 |
| 5:3 | $R_3q^2$ | 2 | 4 | 6:14 | $R_2R_3q^2$ | 4 | 8 |
| 5:4 | $R_3q^2$ | 4 | 8 | 6:15 | $2R_2R_3q^2$ | 2 | 4 |
| 5:5 | $3R_3q^2$ | 2 | 4 | 6:16 | $2R_2R_3q^2$ | 4 | 8 |
| 5:6 | $R_2^2q^2$ | 2 | 4 | 6:17 | $3R_2R_3q^2$ | 2 | 4 |
| 5:7 | $R_2^2q^2$ | 4 | 8 | 6:18 | $3R_2R_3q^2$ | 4 | 8 |
| 5:8 | $2R_2^2q^2$ | 2 | 4 | 6:19 | $R_4q^2$ | 2 | 4 |
| 5:9 | $2R_2^2q^2$ | 4 | 8 | 6:20 | $R_4q^2$ | 4 | 8 |
| 6:1 | $R_6$ | 1 | 1 | 6:21 | $4R_4q^2$ | 2 | 4 |
| 6:2 | $2R_2q^4$ | 2 | 12 | | | | |

$$-\frac{E}{NdJS_0^4}=\frac{R_{-1}}{m}[R_0+R_1(2K)+R_2(2K)^2+(R_3+4q^2)(2K)^3+(R_4+20R_2q^2)(2K)^4$$
$$+(R_5+44q^4+24R_3q^2+36R_2^2q^2)(2K)^5+(R_6+392R_2q^4+28R_2^3q^2+84R_2R_3q^2+28R_4q^2)(2K)^6$$
$$+(R_7+552q^6+128R_2q^5+496R_3q^4+1456R_2^2q^4+32R_5q^2+96R_2R_4q^2+48R_3^2q^2+96R_2^2R_3q^2$$
$$+8W_5q^2)(2K)^7+\cdots\,] \,. \tag{4.9}$$

The corresponding expansion for the free energy $F$ up to the same order is readily evaluated from (4.9) via an integral with respect to $K$:

$$F=\frac{1}{K}\int_0^K E(K)dK \ , \tag{4.10}$$

where we ignored an irrelevant integral constant. If one drops all the terms involving $q$ in this series, one has the same series as (2.7b) which appears in the one-dimensional case. Moreover, in the limit $m\rightarrow\infty$, the internal energy $E$ becomes constantly zero in high-temperature region, because $R_i=O(1)$, $W_i=O(1)$, and $q=O(1/m)$ in the limit $m\rightarrow\infty$. This behavior is consistent with the exact result in the large-$m$ limit which will be treated in Sec. V.

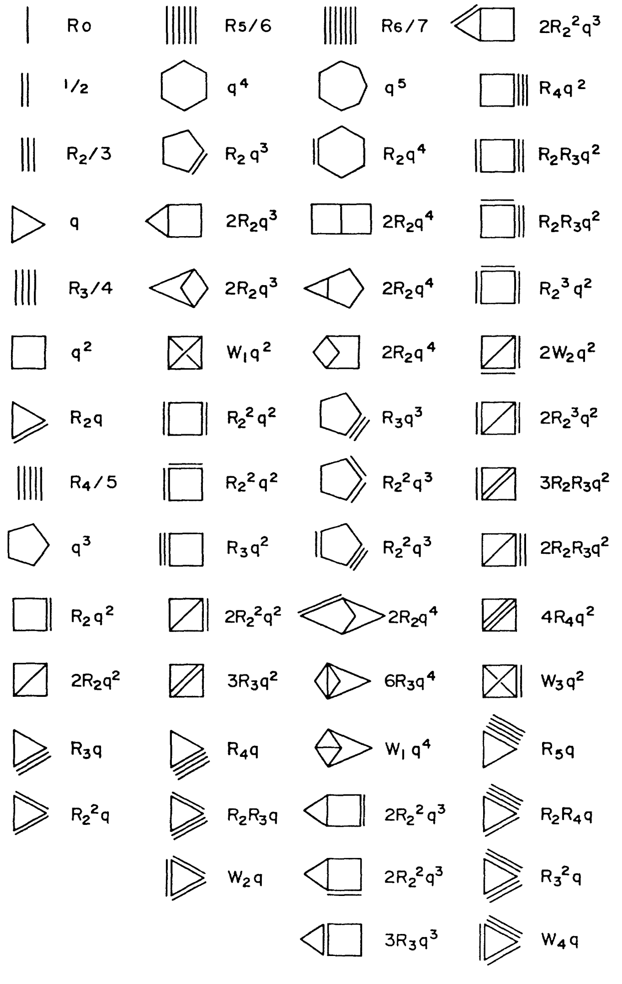

FIG. 7. The free energy diagrams up to the seventh order together with the weight function $m\lambda_l(\mathcal{D})/R_{-1}S_0^4$.

## B. Low-temperature series

At the absolute zero temperature, every axis of the molecules lines up in the same direction, say the $m$th direction. Hence, at extremely low temperatures at $d>2$, deviations of the spins from this direction are so small that one may expand the partition function with respect to these deviations. Let us write the deviations as $\Pi_i=(\Pi_i^1,\Pi_i^2,\ldots,\Pi_i^{m-1})$ for the transverse components and $\sigma_i$ for the longitudinal component. That is, we rewrite the spin variable as

$$\mathbf{S}_i=(\Pi_i^1,\Pi_i^2,\ldots,\Pi_i^{m-1},S_0+\sigma_i) \ , \tag{4.11}$$

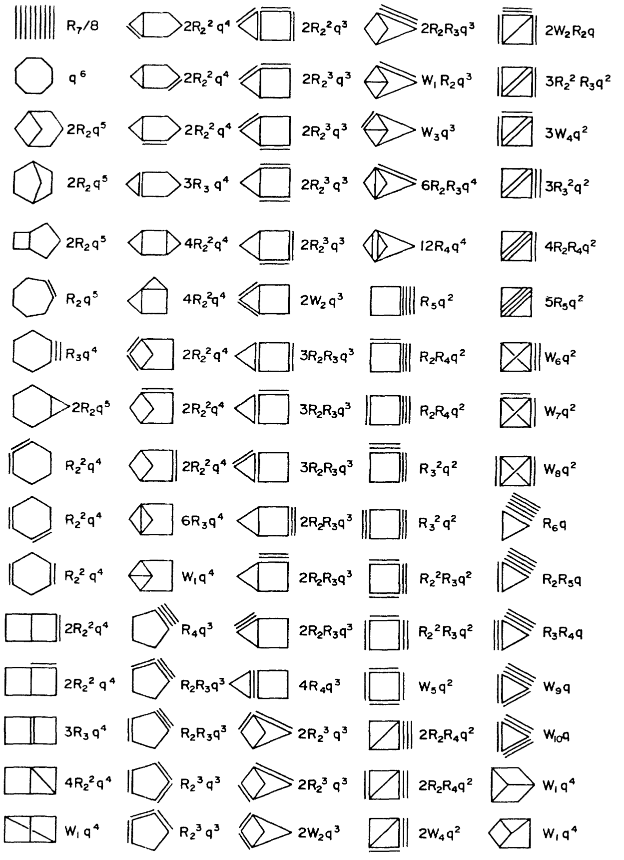

FIG. 8. The free energy diagrams at the eighth order together with the weight function $m\lambda_l(\mathcal{D})/R_{-1}S_0^4$.

TABLE IV. Independent spin-trace functions appearing additionally in the high-temperature series in the higher dimensions.

$$W_1 = -\frac{2(m-2)(m^2+4m-24)}{(m+4)^3}, \qquad W_2 = \frac{2m^6+16m^5-54m^4-181m^3+142m^2+192m-288}{2(m+2)^2(m+4)^2(m+6)^2},$$

$$W_3 = \frac{2(m-1)(m^4+9m^3-37m^2-36m+144)}{(m+2)(m+4)^3(m+6)}, \qquad W_4 = \frac{m(m+1)(m^4+10m^3-59m^2-150m+144)}{(m+2)^2(m+4)^2(m+6)^2(m+8)},$$

$$W_5 = \frac{2m^9+24m^8+37m^7-481m^6-693m^5+2644m^4-804m^3-15984m^2-1728m+20736}{2(m+2)^3(m+4)^3(m+6)^3},$$

$$W_6 = \frac{2(m-2)(m^5+11m^4-85m^3+40m^2+504m-576)}{(m+2)(m+4)^3(m+6)(m+8)},$$

$$W_7 = \frac{(m-2)(2m^5+33m^4-161m^3+42m^2+720m-864)}{(m+2)(m+4)^3(m+6)^2},$$

$$W_8 = \frac{2m^9+40m^8+96m^7-1038m^6-1465m^5+7820m^4+1988m^3-36144m^2-5184m+48384}{(m+2)^3(m+4)^3(m+6)^3},$$

$$W_9 = \frac{2m^{10}+30m^9-173m^8-1728m^7+216m^6+17214m^5+15964m^4-29904m^3-42784m^2-8832m+46080}{2(m+2)^3(m+4)^3(m+6)^2(m+8)(m+10)},$$

$$W_{10} = \frac{(m-2)(m^7+14m^6-113m^5-292m^4+481m^3+812m^2+1536m-2304)}{(m+2)^2(m+4)^2(m+6)^2(m+8)^2}.$$

where $S_0$ is the spin length, i.e., $S_0=|\mathbf{S}_i|$. The transverse and longitudinal components are not mutually independent but related to each other via a relation

$$\sigma_i=\sqrt{S_0^2-\mathbf{\Pi}_i^2}-S_0\ . \tag{4.12}$$

The square of the spin products is then expanded to give

$$\begin{aligned}(\mathbf{S}_i\cdot\mathbf{S}_j)^2=&S_0^4-S_0^2[\mathbf{\Pi}_i^2+\mathbf{\Pi}_j^2-2\mathbf{\Pi}_i\cdot\mathbf{\Pi}_j]\\&-(\mathbf{\Pi}_i^2+\mathbf{\Pi}_j^2)(\mathbf{\Pi}_i\cdot\mathbf{\Pi}_j)\\&+[\mathbf{\Pi}_i^2\mathbf{\Pi}_j^2+(\mathbf{\Pi}_i\cdot\mathbf{\Pi}_j)^2]+\cdots\ .\end{aligned} \tag{4.13}$$

Then the partition function corresponding to the system Hamiltonian (1.4) is given by

$$\begin{aligned}Z_{\text{quadrupole}}&=\frac{\int\exp\left[\frac{J}{T}\sum_{\substack{\langle ij\rangle\\(1\le i,j\le N)}}(\mathbf{S}_i\cdot\mathbf{S}_j)^2\right]\prod_{i=1}^{N}\delta(S_0^2-|\mathbf{S}_i|^2)d\mathbf{S}_i}{\int\prod_{i=1}^{N}\delta(S_0^2-|\mathbf{S}_i|^2)d\mathbf{S}_i}\\&=\frac{\int\prod_{i}^{N}d\mathbf{\Pi}_i\frac{1}{\left[1-\left[\frac{\mathbf{\Pi}_i}{S_0}\right]^2\right]^{1/2}}\exp\left[\frac{J}{T}\sum_{\langle ij\rangle}^{N}(\mathbf{S}_i\cdot\mathbf{S}_j)^2\right]}{\int\prod_{i}^{N}d\mathbf{\Pi}_i\frac{1}{\left[1-\left[\frac{\mathbf{\Pi}_i}{S_0}\right]^2\right]^{1/2}}}\end{aligned} \tag{4.14}$$

where $(\mathbf{S}_i\cdot\mathbf{S}_j)^2$ should be read as (4.13). Since a change of the interval of the $\mathbf{\Pi}_i$ integration from $(-1,1)$ to $(-\infty,\infty)$ affects only the correction of order $\exp(-1/T)$, the low-temperature expansion can be asymptotically performed with the infinite integral. Then expanding around the quadratic (Gaussian) part we find

$$
\begin{aligned}
Z_{\text{quadrupole}} &= \exp\left[\frac{J}{T}\sum_{\substack{\langle ij\rangle\\(1\le i,j\le N)}} S_0^4\right] Z_0(1,1)\left[1+\frac{1}{2S_0^2}\sum_{i=1}^{N}\langle \mathbf{\Pi}_i^2\rangle\right.\\
&\qquad\left.+\frac{J}{T}\sum_{\substack{\langle ij\rangle\\(1\le i,j\le N)}}\langle \mathbf{\Pi}_i^2\mathbf{\Pi}_j^2+(\mathbf{\Pi}_i\cdot\mathbf{\Pi}_j)^2-(\mathbf{\Pi}_i^2+\mathbf{\Pi}_j^2)(\mathbf{\Pi}_i\cdot\mathbf{\Pi}_j)\rangle+\cdots\right]\\
&= \exp\left[\frac{J}{T}\sum_{\substack{\langle ij\rangle\\(1\le i,j\le N)}} S_0^4\right] Z_0(1,1)\left[1+\frac{m-1}{2S_0^2}\sum_{i=1}^{N}\langle \Pi_i^1\Pi_i^1\rangle\right.\\
&\qquad+\frac{(m-1)J}{T}\sum_{\substack{\langle ij\rangle\\(1\le i,j\le N}}[m\langle \Pi_i^1\Pi_i^1\rangle\langle \Pi_j^1\Pi_j^1\rangle+(m+2)\langle \Pi_i^1\Pi_j^1\rangle^2\\
&\qquad\left.-2(m+1)\langle \Pi_i^1\Pi_i^1\rangle\langle \Pi_i^1\Pi_j^1\rangle]+\cdots\right]. \qquad (4.15)
\end{aligned}
$$

Here we introduced notations

$$
Z_0(\alpha,\beta)=\int\prod_{i=1}^{N}d\mathbf{\Pi}_i\exp\left[-\frac{JS_0^2}{T}\sum_{\substack{\langle ij\rangle\\(1\le i,j\le N)}}[\alpha(\mathbf{\Pi}_i^2+\mathbf{\Pi}_j^2)-2\beta(\mathbf{\Pi}_i\cdot\mathbf{\Pi}_j)]\right], \qquad (4.16)
$$

$$
\langle\cdots\rangle=\frac{1}{Z_0}\int\prod_{i=1}^{N}d\mathbf{\Pi}_i\cdots\exp\left[-\frac{JS_0^2}{T}\sum_{\substack{\langle ij\rangle\\(1\le i,j\le N)}}[(\mathbf{\Pi}_i^2+\mathbf{\Pi}_j^2)-2(\mathbf{\Pi}_i\cdot\mathbf{\Pi}_j)]\right], \qquad (4.17)
$$

and used Wick's theorem for the Gaussian variables. Let us assume the $d$-dimensional hypercubic lattice. By means of the Fourier decomposition

$$
\mathbf{\Pi}_n=\frac{1}{\sqrt{N}}\sum_{\mathbf{q}}\tilde{\mathbf{\Pi}}_{\mathbf{q}}e^{i\mathbf{q}\cdot\mathbf{n}}, \qquad (4.18)
$$

the related functions are evaluated as

$$
Z_0(\alpha,\beta)=\left[\frac{\Gamma(m/2)}{\pi^{m/2}}\right]^N\prod_{\mathbf{q}}\left[\frac{\pi T}{[2JS_0^4\{\alpha d-\beta\sum_{i=1}^{d}\cos q_i\}]}\right]^{(m-1)/2}, \qquad (4.19)
$$

$$
\langle \Pi_i^1\Pi_i^1\rangle=-\frac{T}{2Nd(m-1)S_0^2}\frac{\partial}{\partial\alpha}\ln Z_0(\alpha,1)|_{\alpha=1}=\frac{T}{4NJS_0^2}\sum_{\mathbf{q}}\frac{1}{d-\sum_{i=1}^{d}\cos q_i}, \qquad (4.20)
$$

and

$$
\langle \Pi_i^1\Pi_j^1\rangle=-\frac{T}{2Nd(m-1)S_0^2}\frac{\partial}{\partial\beta}\ln Z_0(1,\beta)\bigg|_{\beta=1}=\frac{T}{4NJS_0^2}\sum_{\mathbf{q}}\frac{\sum_{i=1}^{d}\cos q_i}{d-\sum_{i=1}^{d}\cos q_i}=\langle \Pi_i^1\Pi_i^1\rangle-\frac{T}{4dJS_0^2}. \qquad (4.21)
$$

Here and for later use in Sec. V, it is convenient to introduce two integrals,

$$
\Phi_d(\xi)=\frac{1}{N}\sum_{\mathbf{q}}\ln\left[d-\sum_{i=1}^{d}\cos q_i+\xi\right] \qquad (4.22a)
$$

and

$$
\Psi_d(\xi)=\frac{1}{N}\sum_{\mathbf{q}}\frac{1}{d-\sum_{i=1}^{d}\cos q_i+\xi}, \qquad (4.22b)
$$

where the limit $\xi\to 0$ is taken later. Especially, for a simple cubic lattice ($d=3$), the related integral is evaluated numerically, in the limit $N\to\infty$ and $\xi\to 0$, by use of an integral representation with the exponential and the modified Bessel function[17,23] to give

$$
\Phi_3(0)=0.9803,\quad \Psi_3(0)=0.5044. \qquad (4.22c)
$$

Combining (4.15) and (4.19)–(4.22a) we finally find

$$\frac{F}{N\,dJS_0^4}=-1-\frac{T}{dJS_0^4}\ln\left[\frac{\Gamma(m/2)}{\sqrt{\pi}}\left[\frac{T}{2JS_0^4}\right]^{(m-1)/2}\right]+\frac{(m-1)T\Phi_d(0)}{2\,dJS_0^4}-\frac{(m-1)T}{2\,dJS_0^6}\langle\Pi_i^1\Pi_i^1\rangle$$
$$-\frac{(m-1)}{S_0^4}[m\langle\Pi_i^1\Pi_i^1\rangle\langle\Pi_j^1\Pi_j^1\rangle+(m+2)\langle\Pi_i^1\Pi_j^1\rangle^2-2(m+1)\langle\Pi_i^1\Pi_i^1\rangle\langle\Pi_i^1\Pi_j^1\rangle]+\cdots$$
$$=-1-\frac{m}{dK}\ln\left[\frac{\Gamma(m/2)}{\sqrt{\pi}}\left[\frac{m}{2K}\right]^{(m-1)/2}\right]+\frac{(m-1)\Phi_d(0)}{2m\,dK}-\frac{(m-1)(m+2)}{16m^2d^2K^2}+\cdots \tag{4.23}$$

for the free energy and

$$\frac{E}{N\,dJS_0^4}=-1+\frac{m-1}{2m\,dK}+\frac{(m-1)(m+2)T^2}{16m^2d^2K^2}+\cdots \tag{4.24}$$

for the internal energy. Here we put $K=JS_0^4/mT$. It should be emphasized that these expansions are valid only for $d>2$ and do not reproduce the low-temperature series of the exact result at $d=1$. However, it is interesting to note that, for $m=3$ and $d=2$, (4.24) agrees with the result using a normalization group.[12]

We show in Fig. 9 the curves of free and internal energies obtained by the low-temperature series as well as the high-temperature series in three dimensions. A phase transition occurs at the intersection of high- and low-temperature curves of the free energy. The loop surrounded by high- and low-temperature curves of the internal energy may be regarded as a hysteresis loop, because elongations of these two curves correspond to metastable phases. For $m=2$, the high-temperature curve touches the low-temperature curve tangentially in the free energy and the former takes over the latter without jump of slope nearly at the right intersection of the two internal energies. Thus we have a continuous phase transition without hysteresis for $m=2$. On the other hand, for larger values of $m$, the intersection in the free energies lies at a point, where the internal energy shows a jump inside the hysteresis loop. Therefore we expect a first-order phase transition generally for $m>2$. From Fig. 9 we may deduce following results. The transition temperature $T_c \sim 1/K_c$ decreases monotonically with increasing $m$. The discontinuity $\Delta E_c$ in the internal energy first increases with $m$ because the transition point shifts from the right intersection to the bulge, in the hysteresis energy loop; after exceeding a maximum at very large value of $m$, say $m^*$, $\Delta E_c$ becomes decreasing toward some finite value at $m=\infty$ because the transition point shifts in the direction of the left intersection of the hysteresis loop. It is possible to deduce from this analysis the transition point $K_c$ and the amount of the discontinuity $\Delta E_c$ in the internal energy, although an error of estimates would depend on the convergency of the present series. The direct use of the truncated series (Fig. 9), without using any Borel- or Padé-type resummations, offers a crude estimate for $K_c$ and $\Delta E_c$ and the resulting values are tabulated in Table V, in which the exact result in the $m \to \infty$ limit derived in the next section is listed together.

## V. EXACT SOLUTION IN THE $m \to \infty$ LIMIT

Recently, Kunz and Zumbach[14] solved the $m \to \infty$ limit of the lattice $\mathrm{RP}^{m-1}$ model exactly, in the context of particle physics. In this section we reanalyze this problem in terms of the quadrupolar model (1.4) by explicitly taking account of the effect of symmetry breaking fields (1.5) and (1.7). We found that the $m \to \infty$ quadrupolar spin model is characterized by two kinds of order parameters. One is the standard quadrupolar order parameter

$$\Delta^{\mu\nu} \to \langle S_i^\mu S_i^\nu \rangle, \quad \text{as } m \to \infty\ . \tag{5.1}$$

The original definition of $\Delta^{\mu\nu}$ is given in (1.6). In the following we seek it in the form $\Delta^{\mu\nu}=\Delta(1-\delta_{\mu\nu})$. By diagonalization, one may see that this choice of the order parameter is equivalent to our previous choice (3.11). The other order parameter, which we call the bond order parameter $\Delta_2$, is peculiar to the $m \to \infty$ limit and has no counterpart in the case of finite $m$. It is defined at each *bond* via

$$\Delta_2=\frac{1}{m}|\langle \mathbf{S}_i \cdot \mathbf{S}_j \rangle|\ , \tag{5.2}$$

where $i$ and $j$ denote two sites next to each other. One can immediately see that $\Delta_2$ is trivially zero for any finite $m$, since, under a local transformation $\mathbf{S}_i \to -\mathbf{S}_i$, the Hamiltonian (1.4) is invariant while $\langle \mathbf{S}_i \cdot \mathbf{S}_j \rangle$ changes sign. In the $m \to \infty$ limit, however, this is no longer the case. The above transformation for a single spin now involves *infinite degrees of freedom* and virtually concerns a *global symmetry*. Therefore, in the $m \to \infty$ limit, and in this limit only, $\Delta_2$ could be finite as a result of a symmetry breaking. In an ordered state with finite $\Delta_2$, the mutual direction of neighboring spins tends to be fixed as either parallel $\langle \mathbf{S}_i \cdot \mathbf{S}_j \rangle > 0$, or antiparallel $\langle \mathbf{S}_i \cdot \mathbf{S}_j \rangle < 0$. Note that such bond orderings can generally occur in a spatially random manner, as illustrated in Fig. 10(a).

TABLE V. The estimates of the transition point $K_c=JS_0^4/mT_c$ and the energy jump $\Delta E_c$ from the high- and low-temperature series expansions for the simple cubic lattice.

| | | |
|---|---|---|
| $m=3$ | $K_c=0.51$ | $\Delta E_c/3NJS_0^4=0.18$ |
| $m=5$ | $K_c=0.45$ | $\Delta E_c/3NJS_0^4=0.29$ |
| $m=10$ | $K_c=0.42$ | $\Delta E_c/3NJS_0^4=0.38$ |
| $m=50$ | $K_c=0.38$ | $\Delta E_c/3NJS_0^4=0.45$ |
| $m=\infty$ | $K_c=0.3674$ | $\Delta E_c/3NJS_0^4=0.425$<br>$\Delta_c=0.472$ |

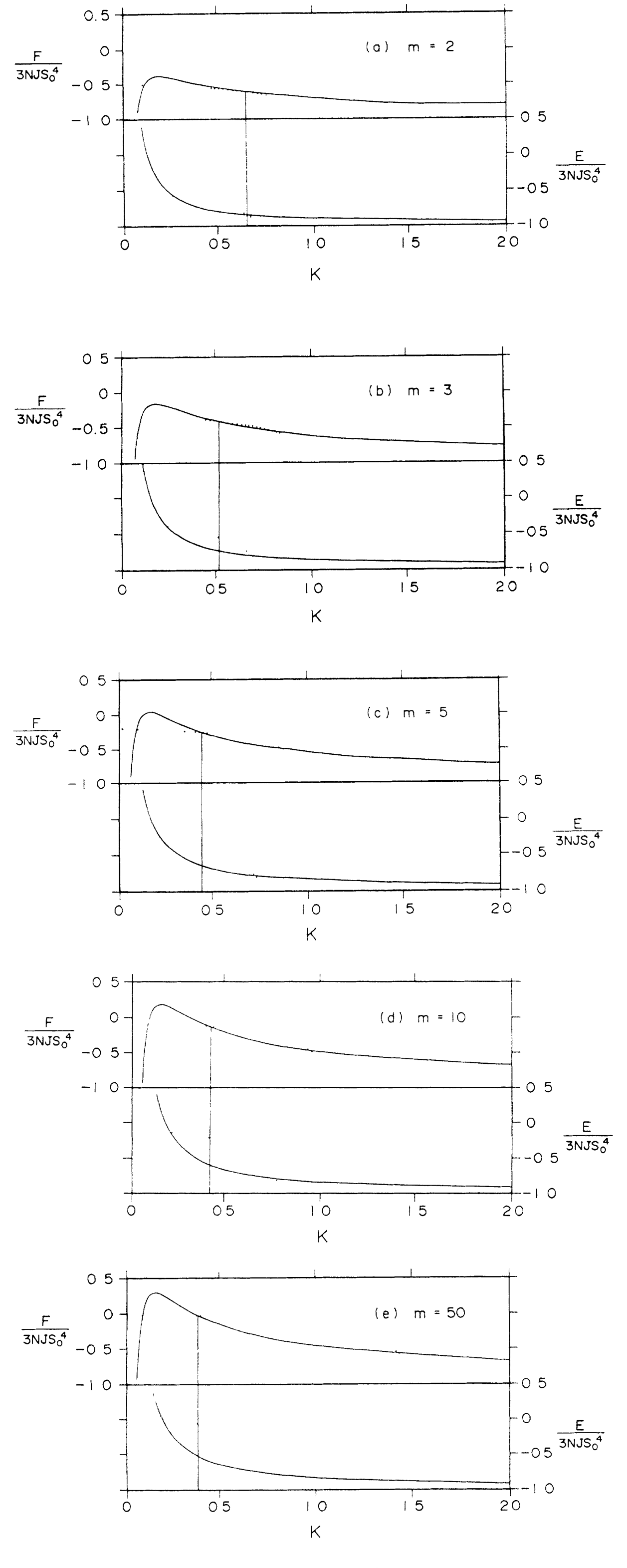

FIG. 9. The free energy $F/3NJS_0^4$ and the internal energy $E/3NJS_0^4$ as a function of $K=JS_0^4/mT$ derived by the high- and low-temperature series expansions for simple cubic lattice ($d=3$); (a) for $m=2$, (b) for $m=3$, (c) for $m=5$, (d) for $m=10$, and (e) for $m=50$. The dotted lines indicate the high-temperature expansion and the solid lines indicate the low-temperature expansion. The phase transition is expected at $K_c$ indicated by a vertical straight line.

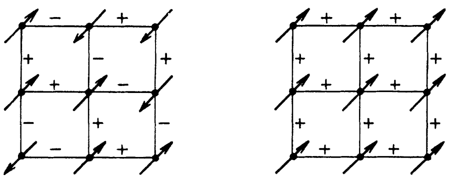

(a) (b)

FIG. 10. Examples of spin configurations realized in ordered states, corresponding to (a) a spatially random case and (b) a uniform case. The signs on each bond, ±, represent the sign of $\langle \mathbf{S}_i\cdot\mathbf{S}_j\rangle$.

Now we sketch our solution. By adding the two kinds of symmetry-breaking terms discussed in Sec. I [see (1.5) and (1.7)], the Hamiltonian is given by

$$\mathcal{H}=-\frac{\tilde{J}}{m}\sum_{\substack{\langle ij\rangle\\(1\le i,j\le N)}}(\mathbf{S}_i\cdot\mathbf{S}_j)^2-\frac{H}{m}\sum_{i=1}^{N}\sum_{\mu,\nu=1}^{m}S_i^\mu S_i^\nu-G\sum_{\substack{\langle ij\rangle\\(1\le i,j\le N)}}\tau_i\tau_j\mathbf{S}_i\cdot\mathbf{S}_j\ , \tag{5.3}$$

where we rescaled spin variables to be $|\mathbf{S}_i|=\sqrt{m}$ and introduced $\tilde{J}=S_0^4J/m$. Equation (5.3) reduces to (1.4) in the limit $H$, $G\rightarrow 0$. In (5.3) an Ising-like variable defined at each site $\tau_i$ takes the values $\pm 1$ and specifies the way of symmetry breaking concerning the bond-order parameter $\langle \mathbf{S}_i\cdot\mathbf{S}_j\rangle$. In fact, the variable $\tau_i$ can be eliminated from the Hamiltonian if one makes a transformation $\mathbf{S}_i\rightarrow\tau_i\mathbf{S}_i$. This procedure corresponds to choosing a uniform "ferromagnetic" state as a particular ordered state, as given in Fig. 10(b), among infinitely many ordered states with $\langle \mathbf{S}_i\cdot\mathbf{S}_j\rangle\neq 0$. Finally we work with

$$\frac{\mathcal{H}}{T}=-\frac{K}{m}\sum_{\substack{\langle ij\rangle\\(1\le i,j\le N)}}(\mathbf{S}_i\cdot\mathbf{S}_j)^2-\frac{h}{m}\sum_{i=1}^{N}\left[\sum_{\mu=1}^{m}\mathbf{S}_i^\mu\right]^2-g\sum_{\substack{\langle ij\rangle\\(1\le i,j\le N)}}\mathbf{S}_i\cdot\mathbf{S}_j\ , \tag{5.4}$$

$$K=\tilde{J}/T,\quad h=H/T,\quad g=G/T\ . \tag{5.5}$$

In taking the $m\rightarrow\infty$ limit we regard $K$ as a quantity of order unity so that the Hamiltonian is of order $m$. The $m$ dependences of the symmetry-breaking terms are determined so that the contributions to the Hamiltonian match that of the interaction term.

The partition function is defined by

$$Z=\int_{-\infty}^{+\infty}\left[\prod_{i=1}^{N}d\mathbf{S}_i\delta(m-|\mathbf{S}_i|^2)\right]\exp\left[-\frac{\mathcal{H}}{T}\right]$$
$$=\exp(-mNf)\ , \tag{5.6}$$

where $f$ is the free energy per spin and per component divided by the temperature. By applying the Hubbard-Stratonovich transformation (3.5) to the $K$ and $h$ terms in (5.4), and utilizing the standard integral representation of the delta function we get

$$Z=A\int_{-i\infty}^{+i\infty}\left[\prod_{i=1}^{N}d\xi_i'\right]\int_{-\infty}^{+\infty}\left[\prod_{\substack{\langle jk\rangle\\(1\le j,k\le N)}}d\zeta_{jk}\right]\int_{-\infty}^{+\infty}\left[\prod_{i=1}^{N}d\eta_i'\right]\exp\left[m\left[\sum_{i=1}^{N}\xi_i'-\sum_{i=1}^{N}\frac{(\eta_i')^2}{4h}-\sum_{\substack{\langle jk\rangle\\(1\le j,k\le N)}}\frac{\zeta_{jk}^2}{4K}-Nf_0\right]\right], \tag{5.7}$$

where $A$ is a numerical constant while $f_0$ is defined by

$$\exp(-Nf_0)=\int_{-\infty}^{+\infty}\left[\prod_{i=1}^{N}dS_i\right]\exp(-\mathcal{H}_0)\ , \tag{5.8}$$

$$\mathcal{H}_0=-\sum_{\substack{\langle ij\rangle\\(1\le i,j\le N)}}(\zeta_{ij}+g)S_iS_j+\sum_{i=1}^{N}\xi_i'S_i^2-\sum_{i=1}^{N}\eta_i'S_i\ . \tag{5.9}$$

In the $m\to\infty$ limit one can evaluate (5.7) by the method of steepest descent. The saddle-point equations are

$$\begin{aligned}1&=\frac{\partial(Nf_0)}{\partial\xi_i'}\ ,\\ \frac{\zeta_{ij}}{2K}&=-\frac{\partial(Nf_0)}{\partial\zeta_{ij}}\ ,\\ \frac{\eta_i'}{2h}&=-\frac{\partial(Nf_0)}{\partial\eta_i'}\ .\end{aligned} \tag{5.10}$$

In solving (5.10) we restrict ourselves to the spatially uniform solutions $\xi_i'=\xi'$, $\zeta_{ij}=\zeta$, and $\eta_i'=\eta'$ for all $i$ and $\langle ij\rangle$. Under this restriction, $f_0$ is easily calculated by means of the Fourier decomposition $S_{\mathbf{n}}=(1/\sqrt{N})\sum_{\mathbf{q}}\tilde{S}_{\mathbf{q}}\exp(i\mathbf{q}\cdot\mathbf{n})$, to give

$$f_0=\frac{1}{2N}\sum_{\mathbf{q}}\ln\left[\xi'-(\zeta+g)\sum_{i=1}^{d}\cos q_i\right]-\frac{(\eta')^2}{4[\xi'-d(\zeta+g)]}-\tfrac{1}{2}\ln\pi\ . \tag{5.11}$$

It is convenient to introduce new variables $\xi$ and $\eta$ as

$$\xi'=(\xi+d)(\zeta+g),\quad \eta'=h\eta\ . \tag{5.12}$$

In terms of these variables the saddle-point equations (5.10) are written into the form

$$2(\zeta+g)=\Psi_d(\xi)+\tfrac{1}{2}\eta^2(\zeta+g)\ , \tag{5.13a}$$

$$\frac{d}{K}\zeta(\zeta+g)=2(\xi+d)(\zeta+g)-1-\tfrac{1}{2}\xi\eta^2(\zeta+g)\ , \tag{5.13b}$$

$$\eta[\xi(\zeta+g)-h]=0\ . \tag{5.13c}$$

Normalized free energy $f$ is given by

$$f=\tfrac{1}{2}\Phi_d(\xi)+\tfrac{1}{2}\ln(\zeta+g)-(\xi+d)(\zeta+g)+\frac{d}{4K}\zeta^2-\tfrac{1}{2}\ln\pi\ . \tag{5.14}$$

In these equations, $\Phi_d(\xi)$ and $\Psi_d(\xi)=\Phi_d'(\xi)$ are the same functions defined in (4.22). Then the two order parameters $\Delta$ and $\Delta_2$ are given by

$$\Delta\equiv-\frac{\partial f}{\partial h}=\frac{1}{4}\eta^2,\quad \Delta_2\equiv-\frac{\partial f}{\partial g}=\frac{\zeta}{2K}\ . \tag{5.15}$$

On the other hand, normalized internal energy $\epsilon$ is

$$\epsilon\equiv\frac{E}{mN\,d\tilde{J}}=\frac{1}{d}\frac{\partial f}{\partial K}=-\frac{\zeta^2}{4K^2}\ . \tag{5.16}$$

Equations (5.15) and (5.16) form a set of the equation of states in the large-$m$ limit. Here the parameters $\zeta$ and $\eta$ are determined as functions of $K$, $h$, and $g$ via equations (5.13a)–(5.13c).

In order to study the phase-transition behavior of the model we take the limit of vanishing symmetry-breaking fields $h\to0$ and $g\to0$. In this case, the coupled equations (5.13) have the following three types of solutions: (A) $\xi=\infty$ ($\xi'=\frac{1}{2}$), $\zeta=\eta=0$, which means $\Delta=\Delta_2=0$ and corresponds to the paramagnetic state; (B) $\xi\neq0$, $\zeta\neq0$, and $\eta=0$, which means $\Delta=0$ and $\Delta_2\neq0$. We call this state the ordered state I: It has a bond long-range order but has no quadrupolar long-range order; (C) $\xi=0$, $\zeta\neq0$, and $\eta\neq0$, which means $\Delta\neq0$ and $\Delta_2\neq0$. We call this state the ordered state II, which corresponds to the conventional ordered state with both quadrupolar and bond long-range orders. This last solution (II) exists only for $d>2$. Since Kunz and Zumbach[14] did not deal with the bond order explicitly, here we reanalyze the overall nature of the phase transitions by considering $\Delta_2$ as well as $\Delta$.

At high temperatures the paramagnetic solution ($P$) is stable, for which the internal energy is always zero, $\epsilon=0$. This conclusion is rather transparent from the nature of the high-temperature expansion developed in Sec. IV A. That is, *in the high-temperature series, all the terms diminish as 1/m or more rapidly, in the $m\to\infty$ limit.* As far as the high-temperature side ($T>T_c$) is concerned, therefore, $\epsilon$ becomes constantly zero in the $m\to\infty$ limit. On decreasing temperature. The solution $P$ becomes unstable against the solution I. This $P$-I instability is described by the equation

$$\begin{aligned}\frac{1}{K}&=\frac{4}{d}\frac{[\Psi_d^{-1}(2\zeta)+d](2\zeta)-1}{(2\zeta)^2}\\ &\simeq2[1+\tfrac{1}{2}(d-\tfrac{3}{2})(2\zeta)^2]+O(\zeta^4)\ ,\end{aligned} \tag{5.17a}$$

where $\Psi_d^{-1}$ denotes the inverse function of $\Psi_d$, since

$$\begin{aligned}\Psi_d(\xi)=\frac{1}{\xi}-\frac{d}{\xi^2}+\frac{d(d+\frac{1}{2})}{\xi^3}-\frac{d^2(d+\frac{3}{2})}{\xi^4}\\ +\frac{d(d^3+3d^2+\frac{3}{4}d-\frac{3}{8})}{\xi^5}\\ -\frac{d^2(d^3+5d^2+\frac{15}{4}d-\frac{15}{8})}{\xi^6}+O\left[\frac{1}{\xi^7}\right]\end{aligned} \tag{5.17b}$$

and

$$\Psi_d^{-1}(2\zeta)=\frac{1}{2\zeta}\left[1-d(2\zeta)+\frac{d}{2}(2\zeta)^2+\frac{d}{4}\left[d-\frac{3}{2}\right](2\zeta)^4+O(\zeta^6)\right] . \tag{5.17c}$$

From (5.17a) one can see that the $P$-I instability occurs at $K_c=\frac{1}{2}$ and that the associated phase transition is continuous for $d\leq\frac{3}{2}$ but should be first order for $d>\frac{3}{2}$ because it becomes impossible to assume $\zeta=+0$ at $K=K_c+0$. At lower temperatures and for $d>2$, the solution I becomes unstable against the solution II, for which,

$$\zeta=K\left[1+\left[1-\frac{1}{dK}\right]^{1/2}\right] , \tag{5.18a}$$

$$\eta=2\sqrt{1-\tfrac{1}{2}d\Psi_d(0)[1-(1-1/dK)^{1/2}]} . \tag{5.18b}$$

When more than one solution are possible at a given temperature, that giving the lowest free energy must be chosen. The resulting phase transition behavior has turned out to be rather rich, depending on the spatial dimensionality sensitively.

(i) $d\leq\frac{3}{2}$. There is a single continuous transition at $K_c=\frac{1}{2}$ between a paramagnetic phase ($\Delta=\Delta_2=0$) and an ordered phase I ($\Delta=0$, $\Delta_2\neq 0$). The exponents take the classical values $\alpha=0$ and $\beta_2=\frac{1}{2}$ for $d<\frac{3}{2}$, where the exponent $\beta_2$ pertains to $\Delta_2$. Note that this classical transition persists even for $d=0$ (two isolated spins). At $d=1$, in particular, the internal energy and the bond-order parameter at $K>K_c$ are calculated to be

$$\epsilon=-\left[1-\frac{1}{2K}\right] , \tag{5.19a}$$

$$\Delta_2=\left[1-\frac{1}{2K}\right]^{1/2} . \tag{5.19b}$$

The result (5.19a) is consistent with the one-dimensional exact solution (2.9). At $d=\frac{3}{2}$, the transition becomes tricritical with the classical tricritical exponents $\alpha=\frac{1}{2}$ and $\beta_2=\frac{1}{4}$.

(ii) $\frac{3}{2}<d\leq 2$, *including* $d=2$. Now the transition between the paramagnetic phase and the ordered phase I is of first order with a discontinuity in $\Delta_2$. The quadrupolar order parameter $\Delta$ is still zero at any temperature.

(iii) $2<d<d^*$, *with* $d^*<3$. In this case, two distinct transitions take place, as was pointed out by Kunz and Zumbach.[14] The upper transition between the paramagnetic phase and the ordered phase I is of first order, while the lower transition between ordered phases I and II is continuous with the exponents $\beta=1$ and $\alpha=0$. The occurrence of such successive phase transitions in intermediate dimensions is analogous to the ones found for the transverse-spin-density-wave transition in the $m\rightarrow\infty$ limit.[24]

(iv) $d>d^*$, *including* $d=3$. There is a single first-order transition between the paramagnetic phase and the ordered phase II ($\Delta\neq 0$, $\Delta_2\neq 0$), with discontinuities both in $\Delta$ and $\Delta_2$. The internal energy and the two order parameters in the low-temperature phase are calculated to be

$$\epsilon=\frac{1}{4dK}-\frac{1}{2}\left[1+\left[1-\frac{1}{dK}\right]^{1/2}\right] , \tag{5.20a}$$

$$\Delta=1-\tfrac{1}{2}d\Psi_d(0)\left[1-\left[1-\frac{1}{dK}\right]^{1/2}\right] , \tag{5.20b}$$

$$\Delta_2=\frac{1}{2}\left[1+\left[1-\frac{1}{dK}\right]^{1/2}\right] , \tag{5.20c}$$

which are certainly consistent with the result of our low-temperature series up to the second order (see Sec. IV B) if we take the $m\rightarrow\infty$ limit in the series. The transition point $K_c$ is determined by the equation

$$\Phi_d(0)+\ln\left\{2K_c\left[1+\left[1-\frac{1}{dK_c}\right]^{1/2}\right]\right\}+\frac{1}{2}-dK_c\left[1+\left[1-\frac{1}{dK_c}\right]^{1/2}\right]=0 . \tag{5.21}$$

At $d=3$, Eq. (5.21) is solved numerically by use of Eq. (4.22c), to yield

$$K_c\simeq 0.3674 \tag{5.22}$$

while discontinuities in the internal energy and the two order parameters are estimated to be

$$\Delta\epsilon_c\simeq 0.425,\quad \Delta_c\simeq 0.472,\quad \Delta_{2c}\simeq 0.652 . \tag{5.23}$$

The estimate of $\Delta\epsilon_c$ seems to be consistent with the estimate by Kunz and Zumbach,[14] $3\Delta\epsilon_c\simeq 1.3$. The $K$ dependence of the two order parameters $\Delta$ and $\Delta_2$, are displayed in Fig. 11.

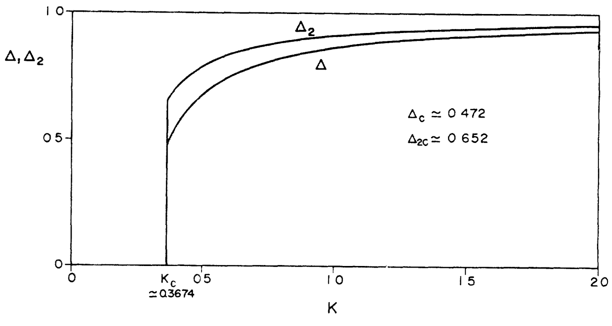

FIG. 11. The $K$ dependence of the order parameters $\Delta$ and $\Delta_2$ of the $m\rightarrow\infty$ model in three dimensions. The corresponding exact expressions are given by (5.20b) and (5.20c), with $K_c\simeq 0.3674$, $\Delta_c\simeq 0.472$, and $\Delta_{2c}\simeq 0.652$.

## VI. SUMMARY AND DISCUSSIONS

First we summarize the main result of this paper. We presented several systematic analyses of the quadrupolar system with general values of $m$ and found that, for $d>2$, the orientational phase transition of the general $m$-component quadrupolar system is first order except for $m=2$.

The model with an infinite-ranged interaction was solved exactly for general values of $m$ and resulted in the revised version of the usual mean-field theory. Especially, we found that the (Landau-type) free-energy expansion up to the fourth order fails down for $m \geq 4$ because the coefficient in the fourth-order term becomes negative for such $m$. This fact may affect some previous results including these free energy expansions.[8,9] The present analysis which does not use the free energy expansion is a reliable one as a mean-field theory for arbitrary $m$. The exact result for the transition point $K_c = JS_0^4/mT_c$ and the discontinuities in the order parameter $\Delta_c$ and in the internal energy $\Delta E_c$ of the infinite-range system are tabulated in Table II as a function of $m$; the transition temperature $T_c$ decreases monotonically with increasing $m$, while the discontinuities $\Delta_c$ and $\Delta E_c$ increase monotonically.

It is now possible to compare the quadrupolar model with the liquid crystal quantitatively. The liquid crystal has been modeled by an ensemble of hard rods which translate and rotate freely in space. At high density the rods undergo a first-order phase transition into the nematic phase, in which the rods are nearly parallel. At the transition the order parameter $\Delta$ is $\Delta_c = 0.85$ in an infinite-dimensional liquid crystal.[19] This is somewhat larger than the typical $\Delta_c$ in a quadrupolar model (see Fig. 4). Therefrom follows that the ordered phase of the quadrupolar model allows more fluctuations and thus is more stable than that of the liquid crystal.

On the other hand, for a short-range system with just the nearest-neighbor interaction of equal strength, we presented an exact solution in one dimension and another exact solution in the $m \rightarrow \infty$ limit. We also presented a high-temperature series up to the seventh order and a low-temperature series up to the second order for general values of $m$. For a simple cubic lattice, the resulting free and internal energies from the expansions were shown in Fig. 9 for several values of $m$; $m=2$, 3, 5, 10, and 50. The value of the transition point $K_c = JS_0^4/mT_c$ and the discontinuity in the internal energy $\Delta E_c$ were tabulated in Table V. The transition point $K_c$ decreases monotonically with increasing $m$, while the discontinuity $\Delta E_c$ first increases with increasing $m$. We may expect similar behavior also in the jump of the order parameter $\Delta_c$. How about the case of quite large values of $m$? Looking at the sequence of figures from small $m$ to large $m$ in Fig. 9, one may anticipate that, after exceeding some quite large value $m = m^*$, which locates at the bulge in the hysteresis loop, $\Delta E_c$ becomes decreasing toward some smaller value at $m = \infty$, and that the large-$m$ limit of this short-range system also undergoes a first-order phase transition. This expectation is certainly consistent with the exact result in the $m \rightarrow \infty$ limit (see Sec. V and the discussion below).

Particular attention was paid for the large-$m$ limit of a short-range case. [For the same limit of an infinite-range case, see discussion from (3.18) to (3.22).] First of all, we explicitly presented the equation of state in this limit; see (5.13)–(5.15). Second we investigated the nature of possible phase transitions. As was discussed in Secs. I and V, there are two order parameters in this limit: one is the usual quadrupolar order parameter $\Delta$ and the other is the bond order parameter $\Delta_2$. The paramagnetic ($P$) solution with $\Delta = \Delta_2 = 0$ is stable at high temperatures. It should be noted that the internal energy is always zero in this phase. This property of vanishing energy turned out to be rather transparent from the point of view of the high-temperature expansion (see the last sentence of Sec. IV A also) if one takes the large-$m$ limit. On decreasing temperature, the $P$ phase becomes unstable against the phase with $\Delta_2 \neq 0$. Such an instability is also a peculiarity in the large-$m$ limit. For $d > d^*$ *with* $2 < d^* < 3$, there is a single first-order transition between the paramagnetic phase and the ordered phase which is characterized by $\Delta \neq 0$ and $\Delta_2 \neq 0$, with discontinuities both in $\Delta$ and $\Delta_2$. The values of $K_c$ and $\Delta E_c$ in three dimensions are also tabulated in Table V. For $2 < d < d^*$, this single transition splits into two successive transitions. The upper transition between the $P$ phase and the ordered phase I characterized by $\Delta = 0$ and $\Delta_2 \neq 0$ is of first order, while the lower transition between the phase I and the phase II which is characterized by $\Delta \neq 0$ and $\Delta_2 \neq 0$ is continuous with the exponents $\beta = 1$ and $\alpha = 0$. On the other hand, for $d \leq 2$, no orientational order appears at any finite temperatures. In this case, there remains the $P$-I transition associated with the order parameter $\Delta_2$. This phase transition is continuous for $d \leq \frac{3}{2}$ and of first order for $d > \frac{3}{2}$.

On the other hand, what happens at $d=2$ for *finite m* is still an interesting issue. A finite-$m$ model is characterized by vanishing order parameters $\Delta = \Delta_2 = 0$ while it can sustain vortex and might exhibit a topological phase transition. In this connection it should be remarked that the existence of a vortex and the possible occurrence of a phase transition in the $m=3$ quadrupolar spin model had been suggested by Solomon.[11] Similar types of vortices were also found in the $m=3$ Heisenberg antiferromagnet on the triangular lattice by Kawamura and Miyashita,[25] who also studied by Monte Carlo simulations the nature of the topological phase transition driven by the vortex dissociation. It has been found that the singularity at the transition is rather weak, clearly not first order. They also argued that the two-point spin correlation function decays exponentially even in the low-temperature phase, and characterized the transition by the changeover observed in the behavior of the "Wilson loop" (vorticity function) between the perimeter-law-like and area-law-like behaviors. In view of similarities between the present quadrupolar spin model and the triangular-lattice Heisenberg antiferromagnetic as to their defect structures, further study is required to clarify the nature of a possible topological phase transition in a quadrupolar model with finite $m$.

Before ending this paper we make a short comment on future problems. Although we restricted ourselves here to the simplest case of the quadrupolar systems, the present analysis may perhaps be applicable to more complicated systems such as quadrupolar glasses, annealed magnets, and systems showing the chiral order. In the forthcoming paper[26] we present an application of the high-temperature series expansion and the infinite-range treatment to the case of quadrupolar glasses with general values of $m$. A higher-order expansion in terms of $1/m$ and a study of the effect of surfaces[21,27] may provide challenging problems also.

## ACKNOWLEDGMENTS

A part of this work was done at Mainz University and K.O. and H.O.C. would like to express their sincere thanks to Professor K. Binder and his co-workers for helpful comments and discussions. They are also grateful to the Alexander von Humboldt Foundation (Bonn, Germany) for financial support. K.O. and Y.O. also thank Professor K. Niizeki for stimulating discussions.

## APPENDIX A

In this appendix we give the derivation of (3.12). Substituting (3.11) into (3.8) with $H^{\mu\nu}=0$ we first obtain

$$f=\frac{(m-1)}{m}\frac{J\Delta^2S_0^4}{2T} -\ln\mathrm{Tr}_1\left\{\exp\left[\frac{J}{T}\Delta S_0^2\left[\phi_1^{11}-\frac{1}{m}\sum_{\mu=1}^{m}\phi_1^{\mu\mu}\right]\right]\right\} . \tag{A1}$$

By using the fact that $\phi_1^{\mu\nu}$ is traceless, the spin trace inside the logarithm in (A1) is evaluated as

$$\begin{aligned}\mathrm{Tr}_1\exp\left[\frac{J\Delta S_0^2}{T}\left[S_1^{(1)}S_1^{(1)}-\frac{S_0^2}{m}\right]\right]&=\mathrm{Tr}_1\exp\left[\frac{J\Delta S_0^4}{T}\left[\cos^2\theta_1-\frac{1}{m}\right]\right]\\ &=\exp\left[(m-1)\frac{J\Delta S_0^4}{mT}\right]\frac{\int_0^{\pi}\sin^{m-2}\theta\exp\left[-\frac{J\Delta S_0^4}{T}\sin^2\theta\right]d\theta}{\int_0^{\pi}\sin^{m-2}\theta\,d\theta}\\ &=\exp\left[(m-1)\frac{J\Delta S_0^4}{mT}\right]{}_1F_1((m-1)/2,m/2;-J\Delta S_0^4/T)\\ &=\exp\left[-\frac{J\Delta S_0^4}{mT}\right]{}_1F_1(\tfrac{1}{2},m/2;J\Delta S_0^4/T) .\end{aligned} \tag{A2}$$

In deriving (A2) we used the integral formula (3.383.1) in Ref. 17 and the self-relation of the confluent hypergeometric function

$$ {}_1F_1(a,b;x)=e^x\,{}_1F_1(b-a,b;-x) . \tag{A3}$$

Thus combining (A1) and (A2) we finally obtain (3.12b). The result (3.12a) for the high-temperature phase is then derived from (3.12b) by setting $\Delta=0$.

## APPENDIX B

We derive the mathematical formula (3.24) in this appendix. We assume the first direction as the $z$ axis and use the polar coordinate in the $m$-dimensional hypersphere. Putting

$$\begin{gathered}S_1^{(1)}=S_0\cos\theta_1,\quad S_1^{(2)}=S_0\sin\theta_1\cos\theta_2 ,\\ \dots ,\\ S_1^{(k)}=S_0\sin\theta_1\cdots\sin\theta_{k-1}\cos\theta_k ,\end{gathered} \tag{B1}$$

we have

$$\begin{aligned}\mathrm{Tr}_1[S_1^{(1)}]^{2l_1}[S_1^{(2)}]^{2l_2}\cdots[S_1^{(k)}]^{2l_k}&=S_0^{2L}\int d\Omega_m\cos^{2l_1}\theta_1\sin^{2(l_2+l_3+\cdots+l_k)}\theta_1\cos^{2l_2}\theta_2\sin^{2(l_3+\cdots+l_k)}\theta_2\times\cdots\\ &\quad\times\cos^{2l_{k-1}}\theta_{k-1}\sin^{2l_k}\theta_{k-1}\cos^{2l_k}\theta_k\Big/\int d\Omega_m ,\end{aligned} \tag{B2}$$

where $L=l_1+l_2+\cdots+l_k$ and $\int d\Omega_m$ denotes the integration over the solid angle on the $m$-dimensional hypersphere. It is convenient to replace (B2) by

$$\begin{aligned}&S_0^{2L}\frac{\int d\Omega_m\cos^{2l_1}\theta_1\sin^{2(l_2+l_3+\cdots+l_k)}\theta_1}{\int d\Omega_m}\frac{\int d\Omega_{m-1}\cos^{2l_2}\theta_2\sin^{2(l_3+\cdots+l_k)}\theta_2}{\int d\Omega_{m-1}}\cdots\\ &\qquad\times\frac{\int d\Omega_{m-k+2}\cos^{2l_{k-1}}\theta_{k-1}\sin^{2l_k}\theta_{k-1}}{\int d\Omega_{m-k+2}}\frac{\int d\Omega_{m-k+1}\cos^{2l_k}\theta_k}{\int d\Omega_{m-k+1}} .\end{aligned} \tag{B3}$$

Using $d\Omega_l=\{2\pi^{l-1}/\Gamma[(l-1)/2]\}\sin^{l-2}\theta\, d\theta$ and the integral formula (3.621.5) in Ref. 17, i.e.,

$$\int_0^{\pi} d\theta\, |\cos\theta|^{\mu-1}\sin^{\nu-1}\theta=B(\mu/2,\nu/2)\ , \tag{B4}$$

we have

$$\mathrm{Tr}_1[S_1^{(1)}]^{2l_1}[S_1^{(2)}]^{2l_2}\cdots[S_1^{(k)}]^{2l_k} =S_0^{2L}\frac{\Gamma(m/2)\Gamma(\frac{1}{2}+l_1)\Gamma(\frac{1}{2}+l_2)\cdots\Gamma(\frac{1}{2}+l_k)}{\pi^{k/2}\Gamma(m/2+L)}\ , \tag{B5}$$

where $B(\alpha,\beta)$ and $\Gamma(\alpha)$ denote the $\beta$ and $\gamma$ functions,[17] respectively. Then, rewriting (B5) with the double factorial $(2l-1)!!$ we obtain (3.24).

## APPENDIX C

This appendix is devoted to prove the two theorems in Sec. IV A. In order to distinguish different bonds we introduce the site-dependent coupling $J_{ij}$ as in (1.3) and use the notation $K_{ij}=J_{ij}S_0^4/mT$ and $\mathcal{H}_{ij}=-J_{ij}(\mathbf{S}_i\cdot\mathbf{S}_j)^2$.

Theorem 1. The expansion coefficient for the free energy corresponding to the diagram $\mathcal{D}$ which has $l_{fg}$ interaction lines on $fg$-bond is written as

$$\lambda_{l+1}(\mathcal{D})=\frac{2S_0^4}{m}\frac{1}{l_{12}!\cdots l_{fg}!\cdots}\left[\left(\frac{\partial}{\partial(2K_{12})}\right)^{l_{12}}\cdots\left(\frac{\partial}{\partial(2K_{fg})}\right)^{l_{fg}}\cdots\ln[\mathrm{Tr}e^{-\mathcal{H}/T}]\right|_{\{J_{ij}\}=0}\ . \tag{C1}$$

Then carrying out one differential with respect to $2K_{fg}$ first we have

$$\begin{aligned}\lambda_{l+1}(\mathcal{D})&=\frac{1}{l_{fg}}\frac{1}{l_{12}!\cdots(l_{fg}-1)!\cdots}\left[\left(\frac{\partial}{\partial(2K_{12})}\right)^{l_{12}}\cdots\left(\frac{\partial}{\partial(2K_{fg})}\right)^{l_{fg}-1}\cdots\frac{\mathrm{Tr}[(\mathbf{S}_f\cdot\mathbf{S}_g)^2e^{-\mathcal{H}/T}]}{\mathrm{Tr}e^{-\mathcal{H}/T}}\right|_{\{J_{ij}\}=0}\\ &=\frac{1}{l_{fg}}\alpha_l(\mathcal{D}_{fg})\ ,\end{aligned} \tag{C2}$$

where $\alpha_l(\mathcal{D}_{fg})$ is the energy coefficient for the diagram $\mathcal{D}_{fg}$ which has one external line and $l_{fg}-1$ interaction lines on $fg$-bond.

Theorem 2. The expansion coefficient for the free energy corresponding to the diagram $\mathcal{D}'$ which has 1, $l_{kj}$, and $l_{ij}-1$ interaction lines, respectively, on $ik$-bond, $kj$-bond, and $ij$-bond, is written as

$$\begin{aligned}\lambda_{l+l_{kj}+1}(\mathcal{D}')&=\frac{2S_0^4}{m}\frac{1}{l_{12}!\cdots l_{kj}!(l_{ij}-1)!\cdots}\\ &\quad\times\left[\left(\frac{\partial}{\partial(2K_{12})}\right)^{l_{12}}\cdots\left(\frac{\partial}{\partial(2K_{ik})}\right)\left(\frac{\partial}{\partial(2K_{kj})}\right)^{l_{kj}}\left(\frac{\partial}{\partial(2K_{ij})}\right)^{l_{ij}-1}\cdots\ln[\mathrm{Tr}e^{-\mathcal{H}/T}]\right|_{\{J_{ij}\}=0}\ .\end{aligned} \tag{C3}$$

First evaluating one differentiation with respect to $2K_{ik}$ we have

$$\begin{aligned}\lambda_{l+l_{kj}+1}(\mathcal{D}')&=\frac{1}{l_{12}!\cdots l_{kj}!(l_{ij}-1)!\cdots}\left[\left(\frac{\partial}{\partial(2K_{12})}\right)^{l_{12}}\cdots\left(\frac{\partial}{\partial(2K_{kj})}\right)^{l_{kj}}\right.\\ &\quad\times\left.\left(\frac{\partial}{\partial(2K_{ij})}\right)^{l_{ij}-1}\cdots\frac{\mathrm{Tr}[S_i^{(n_1)}S_i^{(n_2)}S_k^{(n_1)}S_k^{(n_2)}e^{-\mathcal{H}/T}]}{\mathrm{Tr}e^{-\mathcal{H}/T}}\right|_{\{J_{ij}\}=0}\end{aligned} \tag{C4}$$

In evaluating all the spin traces we may fix the direction of one of the spins, because of the rotational symmetry in spin space. If we fix the spin $\mathbf{S}_j$ to the $\alpha$th direction, then we may perform the spin trace at point $k$ independently as

$$\frac{1}{l_{kj}!}\left[\left(\frac{\partial}{\partial(2K_{kj})}\right)^{l_{kj}}\frac{\mathrm{Tr}_k(S_k^{(n_1)}S_k^{(n_2)}e^{-\mathcal{H}_{kj}/T})}{\mathrm{Tr}e^{-\mathcal{H}_{kj}/T}}\right]_{\{J_{ij}\}=0}$$

$$=\delta_{n_1,\alpha}\delta_{n_2,\alpha}\frac{1}{l_{kj}!}\left[\left(\frac{\partial}{\partial(2K_{kj})}\right)^{l_{kj}}\frac{\mathrm{Tr}_k(S_k^{(\alpha)}S_k^{(\alpha)}e^{-\mathcal{H}_{kj}/T})}{\mathrm{Tr}e^{-\mathcal{H}_{kj}/T}}\right]_{\{J_{ij}\}=0}$$

$$+\delta_{n_1,n_2}(1-\delta_{n_1,\alpha})(1-\delta_{n_2,\alpha})\frac{1}{l_{kj}!}\frac{1}{m-1}\sum_{\beta(\neq\alpha)}\left[\left(\frac{\partial}{\partial(2K_{kj})}\right)^{l_{kj}}\frac{\mathrm{Tr}_k(S_k^{(\beta)}S_k^{(\beta)}e^{-\mathcal{H}_{kj}/T})}{\mathrm{Tr}e^{-\mathcal{H}_{kj}/T}}\right]_{\{J_{ij}\}=0}$$

$$=\left[\delta_{n_1,\alpha}\delta_{n_2,\alpha}-\frac{\delta_{n_1,n_2}(1-\delta_{n_1,\alpha})(1-\delta_{n_2,\alpha})}{m-1}\right]\frac{1}{l_{kj}!}\left[\left(\frac{\partial}{\partial(2K_{kj})}\right)^{l_{kj}}\frac{\mathrm{Tr}_k[S_k^{(\alpha)}S_k^{(\alpha)}e^{-\mathcal{H}_{kj}/T}]}{\mathrm{Tr}e^{-\mathcal{H}_{kj}/T}}\right]_{\{J_{ij}\}=0}$$

$$+\frac{\delta_{n_1,n_2}(1-\delta_{n_1,\alpha})(1-\delta_{n_2,\alpha})}{m-1}\frac{1}{l_{kj}!}\sum_{\beta}\left[\left(\frac{\partial}{\partial(2K_{kj})}\right)^{l_{kj}}\frac{\mathrm{Tr}_k(S_k^{(\beta)}S_k^{(\beta)}e^{-\mathcal{H}_{kj}/T})}{\mathrm{Tr}e^{-\mathcal{H}_{kj}/T}}\right]_{\{J_{ij}\}=0}$$

$$=\left[\left(1+\frac{1}{m-1}\right)\delta_{n_1,\alpha}\delta_{n_2,\alpha}-\frac{\delta_{n_1,n_2}}{m-1}\right]\frac{1}{l_{kj}!}\left[\left(\frac{\partial}{\partial(2K_{kj})}\right)^{l_{kj}}\frac{\mathrm{Tr}_k(S_k^{(\alpha)}S_k^{(\alpha)}e^{-\mathcal{H}_{kj}/T})}{\mathrm{Tr}e^{-\mathcal{H}_{kj}/T}}\right]_{\{J_{ij}\}=0}$$

$$+\frac{\delta_{n_1,n_2}(1-\delta_{n_1,\alpha})(1-\delta_{n_2,\alpha})}{m-1}\frac{1}{l_{kj}!}\left[\left(\frac{\partial}{\partial(2K_{kj})}\right)^{l_{kj}}\frac{\mathrm{Tr}_k(\mathbf{S}_k^2e^{-\mathcal{H}_{kj}/T})}{\mathrm{Tr}e^{-\mathcal{H}_{kj}/T}}\right]_{\{J_{ij}\}=0}$$

$$=\left[\frac{m}{m-1}\delta_{n_1,\alpha}\delta_{n_2,\alpha}-\frac{\delta_{n_1,n_2}}{m-1}\right]\frac{1}{l_{kj}!}\left[\left(\frac{\partial}{\partial(2K_{kj})}\right)^{l_{kj}}\frac{\mathrm{Tr}_k(S_k^{(\alpha)}S_k^{(\alpha)}e^{-\mathcal{H}_{kj}/T})}{\mathrm{Tr}e^{-\mathcal{H}_{kj}/T}}\right]_{\{J_{ij}\}=0}$$

$$=qR_{l_{kj}}S_0^2\left[\delta_{n_1,\alpha}\delta_{n_2,\alpha}-\frac{\delta_{n_1,n_2}}{m}\right], \tag{C5}$$

where we utilized $\mathbf{S}_k^2=S_0^2=\text{constant}$, $q=1/(m+2)$, and (2.5b) of the high-temperature series of the energy in the one-dimensional system. Thus inserting (C5) into (C4) we have

$$\lambda_{l+l_{kj}+1}(\mathcal{D}')=\frac{qR_{l_{kj}}}{l_{12}!\cdots(l_{ij}-1)!\cdots}\left\{\left(\frac{\partial}{\partial(2K_{12})}\right)^{l_{12}}\cdots\left(\frac{\partial}{\partial(2K_{ij})}\right)^{l_{ij}-1}\cdots\right.$$

$$\left.\times\left[\frac{\mathrm{Tr}[(\mathbf{S}_i\cdot\mathbf{S}_j)^2e^{-\mathcal{H}/T}]}{\mathrm{Tr}e^{-\mathcal{H}/T}}-\frac{S_0^2}{m}\frac{\mathrm{Tr}(\mathbf{S}_i^2e^{-\mathcal{H}/T})}{\mathrm{Tr}e^{-\mathcal{H}/T}}\right]\right\}_{\{J_{ij}\}=0}$$

$$=\frac{2S_0^4}{m}\frac{qR_{l_{kj}}}{l_{12}!\cdots l_{ij}!\cdots}\left[\left(\frac{\partial}{\partial(2K_{12})}\right)^{l_{12}}\cdots\left(\frac{\partial}{\partial(2K_{ij})}\right)^{l_{ij}}\cdots\ln[\mathrm{Tr}e^{-\mathcal{H}/T}]\right]_{\{J_{ij}\}=0}$$

$$=l_{ij}qR_{l_{kj}}\lambda_l(\mathcal{D}), \tag{C6}$$

where $\mathcal{D}$ denotes the diagram which has no interaction lines on *ik*-bond and *kj*-bond and $l_{ij}$ interaction lines on *ij*-bond.

---

[*] Present address: Institute for Materials Research, Tohoku University, 2-1-1 Katahira, Aoba-ku, Sendai 980, Japan.

[†] Present address: Fachbereich 1, Universität Bremen, Postfach 330440, D-2800 Bremen, Germany.

[1] W. Maier and A. Saupe, Z. Naturforsch. **14A**, 852 (1959); **15A**, 287 (1960).

[2] S. Hikami and T. Masukawa, Prog. Theor. Phys. **67**, 1038 (1982).

[3] M. Oku and R. Abe, Prog. Theor. Phys. **67**, 118 (1982); M. Oku, *ibid.* **68**, 2176 (1982).

[4] H. O. Carmesin and K. Binder, Z. Phys. **B68**, 375 (1987).

[5] H. O. Carmesin, Z. Phys. **B73**, 381 (1988); H. O. Carmesin and K. Ohno (unpublished).

[6] H. Kawamura, Phys. Rev. B **38**, 4916 (1988).

[7] H. O. Carmesin, Phys. Lett. A **125**, 294 (1987).

[8] P G. de Gennes, Phys. Lett. **30A**, 454 (1969).

[9] T. C. Lubensky and G. Priest, Phys. Lett. **48A**, 103 (1974).

[10] P. A. Lebwohl and G. Lasher, Phys. Rev. A **6**, 426 (1972).

[11] S. Solomon, Phys. Lett. **100B**, 492 (1981).

[12] D. K. Sinclair, Nucl. Phys. **B205** [FS5], 173 (1982).

[13] M. Fukugita, M. Kobayashi, M. Okawa, Y. Oyanagi, and A. Ukawa, Phys. Lett. **109B**, 209 (1982).

[14] H. Kunz and G. Zumbach, J. Phys. **A22**, L1043 (1989).

[15] A. Erdélyi, W. Magnus, F. Oberhettinger, and F. G. Tricomi, *Higher Transcendental Functions* (McGraw-Hill, New York, 1953), Vol. 2, p. 247.

[16] H. E. Stanley, Phys. Rev. **179**, 570 (1969).

[17] I. S. Gradshteyn and I. M. Ryzhik, *Table of Integrals, Series and Products* (Academic, New York, 1965; 1980).

[18] H. O. Carmesin and Y. Fan, J. Phys. (to be published).

[19] H. O. Carmesin, H. L. Frisch, and J. K. Percus, Phys. Rev. B **40**, 9416 (1989).

[20] H. E. Stanley and T. A. Kaplan, Phys. Rev. Lett. **16**, 981 (1966).

[21] H. E. Stanley, in *Phase Transitions and Critical Phenomena*, edited by C. Domb and M. S. Green (Academic, London, 1974), Vol. 3.

[22] K. Ohno, Y. Okabe, and A. Morita, Prog. Theor. Phys. **71**, 714 (1984).

[23] See, for example, R. J. Baxter, *Exactly Solved Models in Statistical Mechanics* (Academic, London, 1982), p. 65.

[24] H. Kawamura, Phys. Rev. B **38**, 960 (1988).

[25] H. Kawamura and S. Miyashita, Prog. Theor. Phys. **53**, 4138 (1984).

[26] H. O. Carmesin and K. Ohno (unpublished).

[27] K. Ohno and Y. Okabe, Prog. Theor. Phys. **70**, 1226 (1983); **72**, 736 (1984).